GPT4SCENE: UNDERSTAND 3D SCENES FROM VIDEOS WITH VISION-LANGUAGE MODELS

Anonymous authors
Paper under double-blind review

ABSTRACT

In recent years, 2D Vision-Language Models (VLMs) have made significant strides in image-text understanding tasks. However, their performance in 3D spatial comprehension, which is critical for embodied intelligence, remains limited. Recent advances have leveraged 3D point clouds and multi-view images as inputs, yielding promising results. However, we propose exploring a purely vision-based solution inspired by human perception, which merely relies on visual cues for 3D spatial understanding. This paper empirically investigates the limitations of VLMs in 3D spatial knowledge, revealing that their primary shortcoming lies in the lack of global-local correspondence between the scene and individual frames. To address this, we introduce GPT4Scene, a novel visual prompting paradigm in VLM training and inference that helps build the global-local relationship, significantly improving the 3D spatial understanding of indoor scenes. Specifically, GPT4Scene constructs a Bird's Eye View (BEV) image from the video and marks consistent object IDs across both frames and the BEV image. The model then inputs the concatenated BEV image and video frames with markers. In zero-shot evaluations, GPT4Scene improves performance over closed-source VLMs like GPT-4o. Additionally, we prepare a processed video dataset consisting of 165K text annotation to fine-tune open-source VLMs, achieving state-of-the-art performance on all 3D understanding tasks. Surprisingly, after training with the GPT4Scene paradigm, VLMs consistently improve during inference, even without object marker prompting and BEV image as explicit correspondence. It demonstrates that the proposed paradigm helps VLMs develop an intrinsic ability to understand 3D scenes, which paves the way for a seamless approach to extending VLMs for 3D scene understanding.

1 INTRODUCTION

3D scene understanding aims to comprehend the overall layout of the surrounding complex environments and the spatial relationships between objects Azuma et al. (2022); Chen et al. (2021; 2020). It plays a crucial role in applications such as embodied intelligence, virtual reality, and smart cities Huang et al. (2023b); Chen et al. (2024b); Chandrasegaran et al. (2024). With the rapid development of Large Language Models Team (2024c); Team & DeepMind (2024); OpenAI (2023); Team (2024d;b), Vision-Language Models have demonstrated impressive performance in image and video understanding Liu et al. (2023; 2024b); Li et al. (2024); Zhu et al. (2023a); Wang et al. (2024a). Researchers have extended this paradigm to 3D perception by incorporating point clouds, aiming to improve scene understanding Hong et al. (2023); Chen et al. (2024b); Wang et al. (2023c); Fu et al. (2024b); Man et al. (2024); Huang et al. (2023b; 2024a); Kang et al. (2024a).

Recent 3D point LLMs leverage point clouds aligned with LLM features for indoor scene understanding Chen et al. (2024b); Hong et al. (2023). While combining point clouds and images Zhu et al. (2024b); Chen et al. (2024b); Huang et al. (2024a) in Point-Vision-LLM paradigms improves performance through richer visual cues, aligning these modalities with text remains challenging. This complexity motivates exploration of vision-only solutions, inspired by humans' natural ability to perceive 3D environments without point clouds, offering a direction for efficient scene analysis.

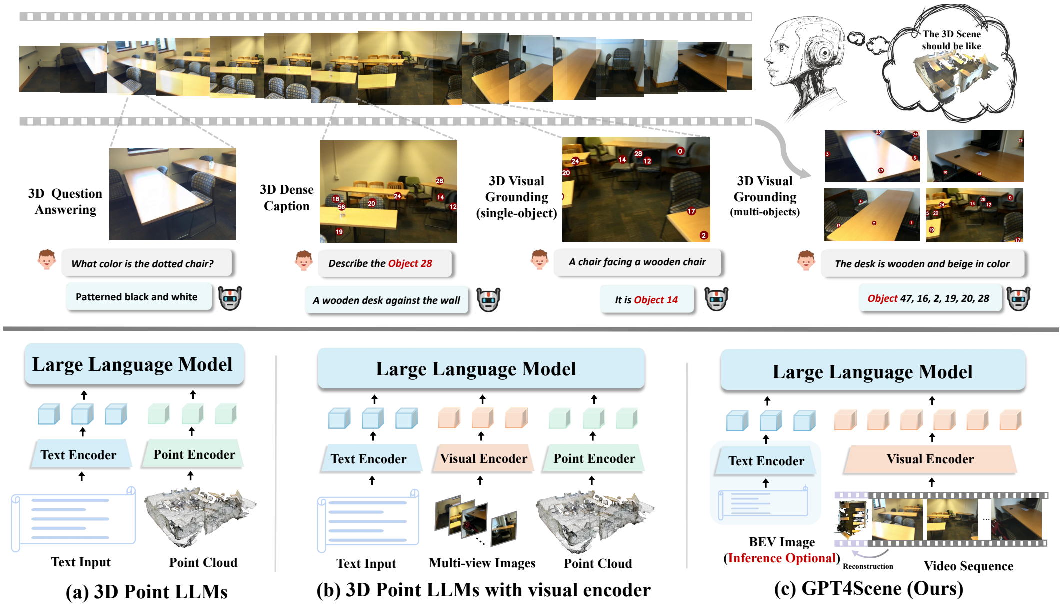

Figure 1: **Overview of GPT4Scene.** GPT4Scene understands 3D scenes and performs tasks like 3D question answering, dense captioning, and visual grounding using only video input. Unlike 3D point LLMs, it relies solely on vision, with global context provided by a BEV image.

In this work, we aim to leverage pre-trained VLMs without modifying their architecture, maximizing their vision perception capabilities. However, their effectiveness in understanding immersive 3D indoor scenes remains limited. Our analysis shows that directly inputting scene videos into VLMs fails in 3D scene understanding due to two factors: i) the lack of a global scene representation, ii) misalignment between per-frame local observations and their spatial-temporal context.

To address this, we propose GPT4Scene, a framework that enhances VLMs' spatial understanding (see Figure 1). We first perform 3D reconstruction on input videos to generate a Bird's Eye View (BEV) image, offering a comprehensive scene layout. Additionally, we introduce Spatial-Temporal Object markers (STO-markers) in both the BEV image and 2D frames. These markers maintain consistent object IDs across frames (temporal level) and align with the BEV image (spatial level), bridging the global-local relationship. Empirical results show that GPT4Scene remains robust to reconstruction quality and marker accuracy, as it prioritizes learning global-local correspondences over precise geometric reconstructions.

We first explored the effectiveness of GPT4Scene under a training-free approach. Experimental results revealed that it was notably effective for powerful large-scale VLMs such as Qwen2-VL-72B Wang et al. (2024a), as well as closed-source models like GPT-4o OpenAI (2024) and Gemini-1.5-Pro Team (2024a), significantly enhancing their 3D scene understanding capabilities, even reaching levels comparable to previous state-of-the-art point-based methods. However, the improvements were limited on smaller-scale models. For smaller open-source vision-language models (VLMs), we introduce ScanAlign, a multimodal dataset comprising 165K aligned data pairs featuring STO-marker-annotated video frames, BEV images, and textual descriptions. Fine-tuning Qwen2-VL-7B on ScanAlign achieves state-of-the-art performance, showing a substantial relative improvement on 3D question answering (SQA3D) and significantly surpassing the previous SOTA, Chat-scene. The model demonstrates even stronger 3D visual grounding capabilities on Multi3DRef, where it also considerably outperforms Chat-scene. These advancements underscore GPT4Scene's effectiveness in seamlessly enhancing VLMs with strong 3D spatial understanding.

Because of the page limit, the related work is shown in **??**.

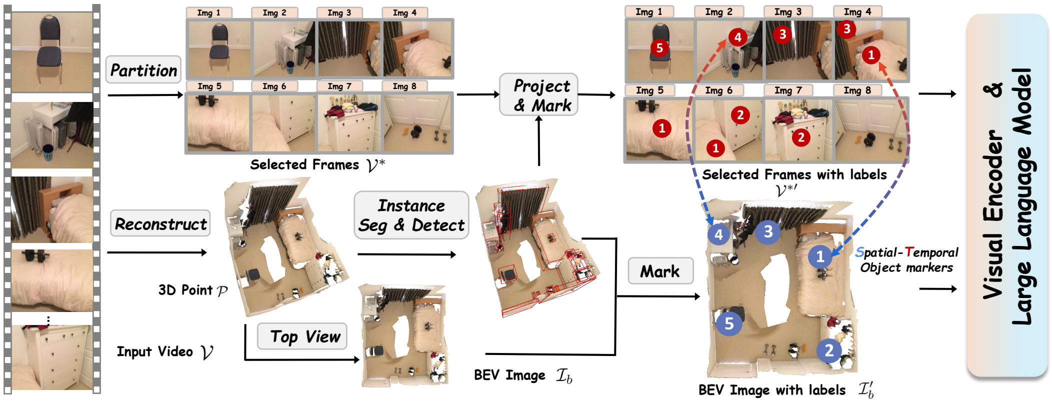
Partition
Img 1
Img 2
Img 3
Img 4
Img 5
Img 6
Img 7
Img 8
Selected Frames $\mathcal{V}^*$
Project & Mark
Selected Frames with labels $\mathcal{V}^{*\prime}$
Reconstruct
3D Point $\mathcal{P}$
Instance Seg & Detect
Top View
Input Video $\mathcal{V}$
BEV Image $\mathcal{I}_b$
Mark
BEV Image with labels $\mathcal{I}_b'$
Spatial-Temporal Object markers
Visual Encoder & Large Language Model

Figure 2: **The framework of GPT4Scene.** A scene video is processed by sampling frames, reconstructing a point cloud, and generating a BEV image. Object locations are detected from the point cloud and projected onto the video frames. The resulting frames and BEV image, enhanced with STO-markers, are inputs for Large Language Model (VLM) training and inference.

Our paper makes these major contributions:

- We introduce GPT4Scene, a framework that enhances Vision-Language Models (VLMs) to comprehend 3D scenes directly from pure vision input.
- We introduce two techniques: i) A 3D BEV image with global context information, and ii) Spatial-Temporal Object markers (STO-markers) for spatial and temporal consistency across BEV image and video frames.
- We introduce ScanAlign, a dataset comprising video frames, BEV images with STO-markers, and text annotations. Fine-tuning VLMs on this dataset significantly improves 3D understanding, even with raw video inputs.
- GPT4Scene demonstrates robust performance in zero-shot and fine-tuning settings, achieving SOTA results across diverse 3D scene understanding tasks.

2 Methodology

We introduce the framework as shown in Subsection 2.1, which improves 3D scene understanding using video inputs. We also explore how zero-shot prompts unlock the potential of large-scale VLMs in Subsection 2.2 and apply fine-tuning for enhanced 3D understanding in Subsection 2.3.

2.1 GPT4Scene Framework

Overview. Here we introduce GPT4Scene's architecture. As shown in fig. 2, our framework combines global scene layouts with object localization details to enhance VLMs' 3D understanding. Given an input video sequence $\mathcal{V} = \{I_1, \dots, I_N\}$ captured during indoor scene traversal, we first reconstruct the 3D scene from the complete video sequence, simultaneously generating a Bird's-Eye View (BEV) map and 3D instance segmentation masks. To establish Spatio-Temporal Object markers (STO-markers), we perform uniform frame sampling by selecting n frames at indices: $s_i = \left\lfloor (i-1)\frac{N}{n} \right\rfloor + 1, \quad \forall i \in \{1, \dots, n\}$ yielding the sampled subset $\mathcal{V}^* = \{I_{s_1}, \dots, I_{s_n}\}$. The 3D instance segmentation results are then projected onto both the BEV map and these keyframes to enable cross-view object localization.

Global information: 3D BEV map. Egocentric videos lack global context, which we address by reconstructing the 3D scene into a point cloud and rendering a bird's-eye view (BEV) image for holistic VLM understanding. Given video $\mathcal{V} = \{I_1, I_2, \dots, I_N\}$ and camera extrinsics $\mathcal{E} = \{E_1, E_2, \dots, E_N\}$, we use 3D reconstruction to generate meshes and point clouds:

$$\mathcal{P} = \mathcal{R}\left(\{(I_t, E_t)\}_{t=1}^{N}\right) \tag{1}$$

$\mathcal{R}(\cdot)$ denotes the reconstruction process, assuming known camera intrinsics. We then generate a BEV image from the global point cloud:

$$\mathcal{I}_b = \mathcal{T}(\mathcal{P},\ E_{top}) \tag{2}$$

Here, $E_{\text{top}} \in \text{SE}(3)$ represents the camera extrinsic for the top-down view, and $\mathcal{T}(\cdot)$ renders the BEV image. We provide global 3D information to VLMs as top-view images rather than points.

Local correspondence: STO-markers. To help VLMs focus on specific objects, we introduce Spatial-Temporal Object markers (STO-markers), ensuring consistency between 2D frames and the 3D BEV image. From the 3D point cloud $\mathcal{P}$ reconstructed from the video $\mathcal{V}$, we apply 3D instance segmentation (e.g., Mask3D) to obtain instance masks $\mathcal{M} = \{M_1, M_2, \ldots M_K\}$, where K is the total number of objects. For the BEV image $\mathcal{I}_{\boldsymbol{b}}$, we project the 3D segmentation masks $\mathcal{M}$ onto the xy plane and extract the center coordinates of the bounding box, $\boldsymbol{C^{xy}} = \{C_1^{xy}, C_2^{xy}, \ldots, C_K^{xy}\}$. These coordinates are then overlaid onto the BEV image. For selected egocentric video frames $\mathcal{V}^*$, the 3D instance masks $\mathcal{M}$ are projected onto each frame based on its camera pose. For each frame i, we extract the centroid of the 2D mask for each object as its 2D marker, $\boldsymbol{C_i^{uv}} = \{C_{i,1}^{uv}, C_{i,2}^{uv}, \ldots, C_{i,K}^{uv}\}$, where $C_{i,k}^{uv}$ is the 2D marker for the k-th object in the i-th frame. The processed frames and BEV image with markers are defined as follows:

$$\mathcal{V}^{*\prime} = \{\mathcal{F}\left(I_i,\ \boldsymbol{C_i^{uv}}\right) \mid i = s_1, s_2, \ldots, s_n\}, \quad \mathcal{I}_b^{\prime} = \mathcal{F}\left(\mathcal{I}_{\boldsymbol{b}},\ \boldsymbol{C^{xy}}\right) \tag{3}$$

Here, $\mathcal{F}(\cdot)$ denotes the STO-marker projection operator that jointly augments both the sampled video frames $\mathcal{V}^*$ and BEV image $\mathcal{I}_b$, producing the marked versions $\mathcal{V}^{*\prime}$ and $\mathcal{I}_b^{\prime}$ respectively. The 2D markers in each frame and their corresponding 3D markers in the BEV image are spatially aligned, ensuring consistency across frames at the object level for temporal coherence.

2.2 The Effectiveness of GPT4Scene in a Zero-Shot Setting

Here, 'zero-shot' refers to the process where we take the original video and, through 3D reconstruction and segmentation, generate a marked Bird's-Eye View (BEV) image and project these markers back onto the 2D video frames. **This results in a video with STO-Markers.** Subsequently, the processed video is fed into the VLM to execute the Question Answering task. As shown in Table 1, our approach had limited impact on smaller models but significantly improved performance for large-scale ones (including the Qwen2-VL-72B, GPT-4o, and Gemini-2.5 Pro), matching the Chat-scene Huang et al. (2024a). These findings indicate the limitations of smaller Vision-Language Models (VLMs) in 3D scene understanding with zero-shot prompting alone, which motivated us to propose the ScanAlign dataset and fine-tune open-source models for enhanced performance.

Table 1: **The zero-shot capability of GPT4Scene.** Video + GPT4Scene Inference without Fine-tuning.

Zero-shot 3D QA	ROUGE@**ScanQA**		EM-1@**SQA3D**	
	VID	+4Scene	VID	+4Scene
3D LLM Based Model	*Pre SOTA*		*Pre SOTA*	
Chat-scene Huang et al. (2024a)	*41.6*		*54.6*	
Open-sourced VLM Based Model				
Qwen2-VL-2B Wang et al. (2024a)	29.5	30.0 +0.5	36.9	36.2 -0.7
Qwen2-VL-7B Wang et al. (2024a)	30.8	33.2 +2.4	42.1	43.1 +1.0
Qwen2-VL-72B Wang et al. (2024a)	32.1	35.1 **+3.0**	41.5	44.0 **+2.5**
Closed-sourced VLM Based Model				
GPT-4o OpenAI (2024)	34.2	39.3 **+5.1**	42.0	44.8 **+2.8**
Gemini-1.5-Pro Team (2024a)	35.1	39.4 **+4.3**	43.5	46.0 **+2.5**

In a zero-shot setting, the model must create a global-local understanding of a 3D scene by fusing local 2D frame features with global BEV (Bird's-Eye View) features. Smaller models, such as Qwen2-VL-2B and Qwen2-VL-7B, are constrained by their parameter scale (typically in the low billions). Their visual encoders and cross-modal fusion capabilities are consequently weaker. They struggle to fully parse the global layout logic from the BEV image (e.g., the relative positions of objects, spatial boundaries) and cannot precisely match the consistency of STO-markers across different frames and the BEV. This leads to a breakdown in the ”global-local association.” For instance, Results show that the small model Qwen2-VL-2B's zero-shot score actually dropped, a clear sign of its ”capability overload. In contrast, large-scale models like Qwen2-VL-72B and GPT-4o possess the architectural complexity to inherently grasp these feature associations, allowing them to form a preliminary 3D cognitive understanding even without any fine-tuning.

2.3 ENHANCING VLMS WITH SCANALIGN FINE-TUNING

The analysis in the previous section indicates that while zero-shot prompting activates spatial awareness in large-scale models, smaller open-source VLMs require explicit fine-tuning to acquire this capability. To this end, we constructed **ScanAlign**, a large-scale instruction-tuning dataset designed to empower 2D VLMs with 3D understanding.

Distinct from raw data collection, ScanAlign unifies and transforms existing high-quality 3D annotations into a novel visual prompting format. We aggregate 165K text-scene pairs from five mainstream benchmarks based on ScanNet Dai et al. (2017a)—ScanQA Azuma et al. (2022), SQA3D Ma et al. (2023), Scan2Cap Chen et al. (2021), ScanRefer Chen et al. (2020), and Multi3DRef Zhang et al. (2023c). While the text annotations are derived from these prior works, our core contribution lies in **reformatting** these purely geometric data entries (point clouds) into a VLM-compatible format $(\mathcal{V}^{*\prime}, \mathcal{I}_b^{\prime}, T)$. Specifically, we augment the original labels by generating synchronized egocentric video frames and projecting Spatial-Temporal Object (STO) markers onto both frames and BEV images.

Table 2: **ScanAlign**: Datasets used for training GPT4Scene (Supervised Fine-Tuning),

Source	Data Type	Task Type	Samples
		Overall Scene-Level	

ScanQA	3D QA	`Spatial Relationship`
		`Object Attribute`
		`Existence & Counting`
			26K

SQA3D	3D QA	`Egocentric Spatial`
		`Navigation`
		`Object Attribute`
			26K

Total			52K
		Object-Level	

Scan2cap	3D Caption	`Object Attributes`
		`Spatial Location`
		`State or Affordance`
			35K

ScanRefer	3D Grounding	`Combined Attributes`
		`Spatial Relations`
		`Unique Attributes`
			41K

Multi3DRef	3D Grounding	`Group Reference`
		`List-based Refer`
		`Relational Refer`
			35K

Total			165K

3 EXPERIMENTS

In this section, we primarily present the experimental results. First, we outline the training details in Subsection 3.1, and subsequently introduce the fine-tuning main results in Subsection 3.2. Finally, Subsection 3.3 details the ablation study, demonstrating the effectiveness of individual components.

3.1 IMPLEMENTATION DETAILS

Our 3D scene understanding benchmark is based on the ScanNet Dai et al. (2017a) dataset and includes three tasks: 3D question answering (ScanQA Azuma et al. (2022) and SQA3D Ma et al. (2023)), 3D dense captioning (Scan2Cap Chen et al. (2021)), and 3D visual grounding (ScanRefer Chen et al. (2020) and Multi3DRef Zhang et al. (2023c)). Our pipeline begins with 3D scene reconstruction using BundleFusion Dai et al. (2017b) to generate dense point clouds, followed by 3D instance segmentation with Mask3D Schult et al. (2023) to extract object-level masks. The segmented 3D objects are then projected to BEV coordinates, while their corresponding masks are mapped to 2D image frames to establish Spatial-Temporal Object (STO) markers. This comprehensive processing framework enables precise cross-modal alignment essential for both dense captioning and visual grounding tasks. For the experiment, we sample N=32 frames per video (512×490 resolution) for all models. Training is done for one epoch with a base learning rate of 5e-6 and cosine annealing, completing in about 6 hours on 8×A100 GPUs.

3.2 FINE-TUNING MAIN RESULTS

We performed fine-tuning exclusively on ScanAlign: using GPT4Scene as the dataset, we fine-tuned InternVL-3 8B Chen et al. (2023c), Qwen2-VL 7B Wang et al. (2024a), and Qwen2.5-VL 8B Team (2024d), and ultimately achieved state-of-the-art (SOTA) results.

3D question answering. The 3D question answering results presented in Table 3 are categorized into three distinct groups: **(1)** conventional task-specific models, **(2)** architectures based on 3D point cloud LLMs, and **(3)** vision-language multimodal LLM systems. Our experimental analysis demonstrates that the baseline Qwen2-VL-7B model without fine-tuning shows constrained capability in 3D QA scenarios. In terms of specific metrics, models fine-tuned using the GPT4Scene framework (based on the ScanAlign dataset) show outstanding performance: Qwen2-VL-7B (GPT4Scene) achieves a BLEU-1 score of 44.4 and a CIDEr score of 96.3 on the ScanQA dataset, along with

Table 3: **Evaluation of 3D question answer on ScanQA Azuma et al. (2022) & SQA3D Ma et al. (2023).**

3D Question Answering	Point Encoder	Vision Encoder	ScanQA (val)					SQA3D (val)	
Methods			BLEU-1	BLEU-4	METEOR	ROUGE	CIDEr	EM-1	EM-R1
Task-Specific Model									
ScanQA Azuma et al. (2022)	✓	✗	30.2	10.1	13.1	33.3	64.9	-	-
SQA3D Ma et al. (2023)	✓	✗	-	-	-	-	-	46.6	-
3D-VLP Jin et al. (2023)	✓	✗	30.5	11.2	13.5	34.5	-	-	-
3D-Vista Zhu et al. (2023b)	✓	✗	-	-	13.9	35.7	-	48.5	-
3D LLM Based Model									
Chat-3D Wang et al. (2023c)	✓	✗	29.1	6.4	11.9	28.5	53.2	-	-
Chat-3D v2 Huang et al. (2023a)	✓	✗	38.4	7.3	16.1	40.1	77.1	-	-
3D-LLM Hong et al. (2023)	✓	✓	39.3	12.0	14.5	35.7	69.4	-	-
LL3DA Chen et al. (2024b)	✓	✗	-	13.5	15.9	37.3	76.8	-	-
PQ3D Zhu et al. (2024b)	✓	✓	-	-	-	-	-	47.1	-
LEO† Huang et al. (2023b)	✓	✓	-	11.5	16.2	39.3	80.0	50.0	52.4
Grounded-3D-LLM Chen et al. (2024c)	✓	✓	-	13.4	-	-	72.7	-	-
Chat-scene Huang et al. (2024a)	✓	✓	43.2	14.3	18.0	41.6	87.7	54.6	57.5
ROSS3D Wang et al. (2025)	✗	✓	49.2	17.9	20.9	**50.7**	**107.0**	63.0	65.7
Vision LLM Based Model									
SceneLLM Fu et al. (2024b)	✗	✓	43.6	12.0	16.6	40.0	80.0	54.2	-
LLaVA-3D Zhu et al. (2024a)	✗	✓	-	14.5	20.7	50.1	91.7	55.6	-
Video-3D-LLM Zheng et al. (2025)	✗	✓	47.1	16.2	19.8	-	102.1	58.6	-
InternVL3-8B (GPT4Scene)	✗	✓	45.1	16.2	19.5	47.8	96.8	61.9	64.5
Qwen2-VL-7B (GPT4Scene)	✗	✓	44.4	15.5	18.9	46.5	96.3	60.6	63.3
Qwen2.5-VL-7B (GPT4Scene)	✗	✓	**49.2**	**19.8**	**21.1**	50.2	105.7	**63.5**	**66.2**

an EM-1 score of 60.6 and an EM-R1 score of 63.3 on the SQA3D dataset; The more powerful Qwen2.5-VL-7B (GPT4Scene) further improves the BLEU-1 score to 49.2 and the CIDEr score to 105.7 on ScanQA, while reaching an EM-1 score of 63.5 and an EM-R1 score of 66.2 on SQA3D. These models not only significantly outperform the untuned baseline VLMs but also comprehensively outperform the previous SOTA models in the 3D point cloud LLM category (e.g., Chat-scene). This fully demonstrates that GPT4Scene—by providing global context through BEV (Bird's-Eye View) images and establishing spatiotemporal consistency via STO-markers—can effectively enhance the 3D spatial reasoning and QA capabilities of VLMs.

3D dense caption. Table 4 presents the primary evaluation for the 3D dense captioning task on the Scan2Cap benchmark. The table contrasts the performance of various models using BLEU-4 and ROUGE scores, evaluated at both a lenient (IoU@0.25) and a strict (IoU@0.5) matching threshold. The key objective is to demonstrate the efficacy of our GPT4Scene framework in enhancing the capability of Vision Language Models (VLMs) for detailed 3D scene description. Our GPT4Scene-integrated Visual LLMs, including Qwen2-VL-7B (GPT4Scene) and Qwen2.5-VL-7B (GPT4Scene), achieve breakthrough performance using only visual inputs (video + BEV images). Specifically, Qwen2.5-VL-7B (GPT4Scene) scores a BLEU-4 of 45.9 and a ROUGE of 67.9 at IoU@0.25, and a BLEU-4 of 44.1 with a ROUGE of 67.1 at IoU@0.5. These results comprehensively outperform the other model classes. This superior performance stems from GPT4Scene's ability to provide global scene context via BEV imagery and maintain spatio-temporal consistency through STO-markers. Consequently, the VLM can precisely ground textual descriptions in 3D scene details without requiring 3D point cloud data, thereby establishing a new state-of-the-art (SOTA) in the field.

3D visual grounding. Table 5 presents the critical evaluation for the 3D visual grounding task, which aims to accurately align textual descriptions with their corresponding objects in 3D space. Using the ScanRefer (single/multi-object grounding) and Multi3DRef (combinatorial multi-object grounding) benchmarks, this analysis validates the enhancement of spatial localization capabilities in Vision Language Models (VLMs) by our GPT4Scene framework. Performance is measured by localization accuracy (Acc@0.25 and Acc@0.5) on ScanRefer and the global F1 score (all F1@0.25 and all F1@0.5) on Multi3DRef. Vision LLMs integrated with GPT4Scene, such as InternVL3-

Table 4: **Evaluation of 3D dense caption on Scan2Cap Chen et al. (2021).** Our results outperform those of existing 3D LLM based models.

3D Dense Caption	IoU@0.25		IoU@0.5	
Methods	BLEU-4	ROUGE	BLEU-4	ROUGE
Task-Specific Model				
Scan2Cap Chen et al. (2021)	34.2	55.3	23.3	44.5
3DJCG Cai et al. (2022)	40.2	59.2	31.0	50.8
X-Trans2Cap Yuan et al. (2022)	35.7	54.7	25.1	45.3
3D-VisTA Zhu et al. (2023b)	36.5	57.6	34.0	54.3
Vote2Cap-DETR Chen et al. (2023b)	39.3	59.3	34.5	54.4
3D LLM Based Model				
LL3DA Chen et al. (2024b)	41.4	59.5	36.8	55.1
PQ3D Zhu et al. (2024b)	–	–	36.0	-
LEO Huang et al. (2023b)	–	–	36.9	57.8
Chat-scene Huang et al. (2024a)	38.2	60.6	36.3	58.1
Grounded 3D-LLM Chen et al. (2024c)	–	–	35.5	-
Robin3D Kang et al. (2024a)	–	–	38.4	–
Ross3D Wang et al. (2025)	–	–	43.4	66.9
Vision LLM Based Model				
LLaVA-3D Zhu et al. (2024a)	–	–	41.1	63.4
Video-3D-LLM Zheng et al. (2025)	–	–	41.3	-
InternVL3-8B (GPT4Scene)	44.1	63.1	41.4	60.3
Qwen2-VL-7B (GPT4Scene)	43.1	61.9	40.6	59.3
Qwen2.5-VL-7B (GPT4Scene)	**45.9**	**67.9**	**44.1**	**67.1**

Table 5: **Evaluation of 3D visual grounding on ScanRefer Chen et al. (2020) and Multi3DRef Zhang et al. (2023c).** Our method reaches state-of-the-art performance over all methods for the 3D visual grounding task.

3D Visual Grounding	ScanRefer		Multi3DRef	
Methods	Acc@0.25	Acc@0.50	all F1@0.25	all F1@0.50
Task-Specific Model				
3DVG-Transformer Zhao et al. (2021)	47.6	34.7	–	25.5
3DJCG Cai et al. (2022)	49.6	37.3	–	26.6
D3Net Chen et al. (2022a)	–	37.9	–	32.2
M3DRef-CLIP Zhang et al. (2023c)	51.9	44.7	42.8	38.4
3D LLM Based Model				
3D-LLM Hong et al. (2023)	30.3	-	-	-
Grounded 3D-LLM Chen et al. (2024c)	47.9	44.1	45.2	40.6
Chat-scene Huang et al. (2024a)	55.5	50.2	57.1	52.4
Ross3D Wang et al. (2025)	61.1	54.4	59.6	54.3
Vision LLM Based Model				
LLaVA-3D Zhu et al. (2024a)	54.1	42.4	-	-
Video-3D-LLM Zheng et al. (2025)	58.1	51.7	58.0	52.7
InternVL3-8B (GPT4Scene)	63.4	57.7	65.5	60.7
Qwen2-VL-7B (GPT4Scene)	62.6	57.0	64.5	59.8
Qwen2.5-VL-7B (GPT4Scene)	**65.6**	**59.5**	**67.3**	**62.8**

Table 6: **Ablation study on the Efficacy of GPT4Scene.** (1) on fully fine-tuned models with GPT4Scene; (2) on pure-video fine-tuned models; (3) in a zero-shot setting without training. Exp conducted on Qwen2-VL-7B.

GPT4Scene Train	GPT4Scene Eval	ScanQA		
		METEOR	ROUGE	CIDEr
✓	✓	**18.9**	**46.5**	**96.3**
✓	✗	18.6	45.9	95.4
(Pure Video SFT) ✗	✓	17.3	43.5	88.2
(Pure Video SFT) ✗	✗	16.7	42.1	85.9
(No training) ✗	✓	14.1	33.2	68.7
(No training) ✗	✗	12.4	30.8	64.7

Table 7: **Ablation Study on BEV Reconstruction Quality.** The quality of BEV reconstruction has a negligible impact on QA performance, since the BEV mainly offers a global overview of the scene.

BEV Reconstruction Quality	ScanQA ROUGE	SQA3D EM-1
BundleFusion (Baseline)	46.5	60.6
SLAM3R, 50-frame intervals	46.1	58.8
100-frame intervals	46.7	**61.3**
200-frame intervals	45.8	59.1
GS-SLAM	46.3	60.7
MAST3R-SLAM	**47.0**	59.5

8B (GPT4Scene) and Qwen2-VL-7B (GPT4Scene), demonstrate breakthrough performance using only visual inputs (video + BEV imagery). For instance, Qwen2-VL-7B (GPT4Scene) achieves an Acc@0.25 of 62.6 on ScanRefer and an all F1@0.25 of 64.5 on Multi3DRef, surpassing the previous SOTA, Chat-scene, by 7.1 and 7.4 points, respectively. Furthermore, our improved Qwen2.5-VL-7B (GPT4Scene) model sets a new state-of-the-art, elevating these scores to 65.6 and 67.3.

GPT score: new evaluation way. We propose a novel GPT Score for 3D QA assessment, using the state-of-the-art 3D LLM Chat-scene Huang et al. (2024a) as the baseline. For our comparison, we selected a total of 1,000 questions from the ScanQA dataset, distributed across six distinct categories: Spatial Relationship, Object Attribute, Existence & Counting, State or Affordance, Group Reference, and Relational Refer. We then prompted GPT-4o OpenAI (2024) to compare the responses from our GPT4Scene-finetuned model against those from Chat-scene. The evaluation revealed a clear pattern: GPT4Scene demonstrates a significant performance advantage in object-centric categories, particularly excelling in tasks related to Relational Refer and Existence & Counting. Conversely, the performance gap in the Spatial Relationship category was not significant, indicating comparable capabilities in that area. These findings strongly suggest that the core strengths of GPT4Scene lie in its enhanced understanding and processing at the object level.

3.3 Ablation Study

In this section, we conduct ablation studies to validate the effectiveness of GPT4Scene. First, we evaluate its robustness, including performance on small objects, followed by analyzing the robustness of STO-markers and reconstruction quality. Next, we perform module-wise ablation to assess individual components. Finally, we investigate the impact of frame intervals and resolution settings.

Table 8: **Ablation on the size of objects.** Comprehension is most effective for large objects, and diminishes for smaller ones.

Connector	ScanQA		
	METEOR	ROUGE	CIDEr
All objects	18.9	46.5	96.3
Small (e.g., alarm clock)	17.2	42.8	91.5
Middle (e.g., chair)	18.7	46.6	95.8
Large (e.g., cabinet)	**19.3**	**47.3**	**97.5**

Table 9: **Ablation study on the BEV and STO-Markers.** Both the BEV Image and STO-markers improve understanding. Performance peaks at an optimal STO-marker size before degrading.

ScanQA	*w/i* BEV Image			*w/o* BEV Image		
	METEOR	ROUGE	CIDEr	METEOR	ROUGE	CIDEr
w/o STO-markers	$17.5_{\downarrow 1.4}$	$43.1_{\downarrow 3.4}$	$90.4_{\downarrow 5.9}$	$16.0_{\downarrow 2.9}$	$40.0_{\downarrow 6.5}$	$84.1_{\downarrow 12.2}$
- size: 30, STO	$18.2_{\downarrow 0.7}$	$45.3_{\downarrow 1.2}$	$93.8_{\downarrow 2.5}$	$16.7_{\downarrow 2.2}$	$42.2_{\downarrow 4.3}$	$87.5_{\downarrow 8.8}$
- size: 40, STO	$\mathbf{18.9}_{\downarrow 0.0}$	$\mathbf{46.5}_{\downarrow 0.0}$	$\mathbf{96.3}_{\downarrow 0.0}$	$17.4_{\downarrow 1.5}$	$43.3_{\downarrow 3.2}$	$90.1_{\downarrow 6.2}$
- size: 50, STO	$18.0_{\downarrow 0.9}$	$44.9_{\downarrow 1.6}$	$93.1_{\downarrow 3.2}$	$16.5_{\downarrow 2.4}$	$41.8_{\downarrow 4.7}$	$86.9_{\downarrow 9.4}$

The effectiveness during training and inference. Table 6 presents an ablation study on the GPT4Scene framework, analyzing the contribution of its components by selectively enabling them during training and inference. The study's key finding is that the fine-tuning process with GPT4Scene is the most critical driver of performance. A model trained this way maintains strong results even without the special inference components (BEV images and STO-markers), demonstrating that it acquires an intrinsic 3D understanding. While training is fundamental, the inference components provide a further enhancement, pushing the model to its peak performance when combined. This study clearly validates the dual effectiveness of the GPT4Scene framework in both empowering the model through training and enhancing its capabilities at inference.

Ablation Study on BEV Reconstruction Quality. This ablation study in Table 7 investigates the impact of BEV (Bird's-Eye View) reconstruction quality on model performance. The central hypothesis is that the BEV's primary role is to provide global scene context, not precise geometric detail. The experiment compared various reconstruction methods (e.g., the baseline BundleFusion, SLAM3R at different frame rates) on the ScanQA and SQA3D benchmarks. The results show that despite variations in reconstruction quality, key performance metrics like ROUGE and EM-1 remained stable with only negligible fluctuations. This strongly confirms that the GPT4Scene framework is robust to the geometric precision of the BEV map, depending on it for overall layout rather than fine-grained accuracy.

Ablation on the size of objects. This ablation study in Table 8 analyzes how object size impacts the model's 3D understanding capabilities by categorizing objects into small, medium, and large. The results reveal a clear positive correlation between object size and performance: the model understands large objects best, performs near the average for medium objects, and is least effective with small objects. This is because larger objects provide more prominent visual features and clearer spatial footprints in video frames and BEV maps, making them easier to ground. Nevertheless, the model maintains a strong baseline performance even on small objects, confirming the overall effectiveness and robustness of the GPT4Scene framework across various object scales.

Ablation study on the BEV and STO-Markers. This ablation study in Table 9 provides a detailed analysis of GPT4Scene's two core components: the BEV image and STO-Markers. The results yield two critical conclusions. First, both the BEV image and STO-Markers are essential for performance and demonstrate a clear synergistic effect. The data shows that removing either component—for instance, removing STO-Markers while keeping the BEV image, or vice versa—causes a significant decline across all key metrics (METEOR, ROUGE, and CIDEr). This confirms that the global scene context provided by the BEV and the spatio-temporal consistency established by STO-Markers are both indispensable for high-fidelity 3D comprehension. Second, the study reveals that there is an optimal size for the STO-Markers. Performance peaked when the marker size was set to 40, while smaller (30) or larger (50) sizes led to a drop in performance. This suggests that the marker scale must be properly adapted to the visual features of objects within the scene to maximize its effectiveness in linking global and local information.

Ablation on the number of input frames and image resolution. Figure 4 visualizes an ablation study that assesses the impact of two key parameters—the number of input frames and image resolution—on model performance across different 3D understanding tasks. The experiment compares two core tasks: 3D Question Answering (QA) and 3D Visual Grounding. The central finding is that these parameters affect the two tasks very differently. Both higher image resolution and an increased number of input frames provide a substantial performance boost for the 3D Visual Grounding task, which relies on precise object localization. In contrast, the same parameter upgrades yield only minimal improvements for the 3D QA task, which involves more general scene comprehension. This result leads to a clear conclusion: for tasks like Visual Grounding, prioritizing high-resolution,

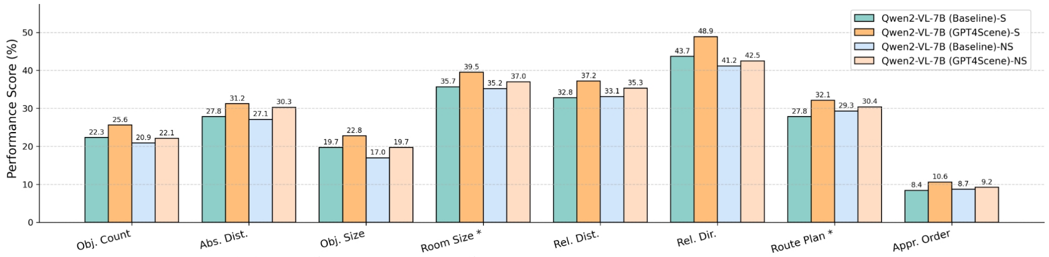

Figure 3: **Evaluation of GPT4Scene on the VSIBench.** ’S’ denotes performance on ScanNet, while ’NS’ refers to the ARKitScenes dataset. The results indicate that GPT4Scene enhances spatial intelligence.

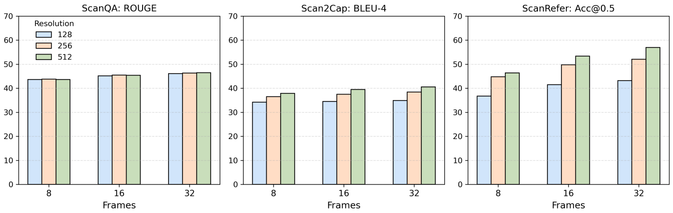

Figure 4: **Ablation on the number of input frames and image resolution.** We find that these parameters have the most significant impact on the Grounding task and the least on question answering.

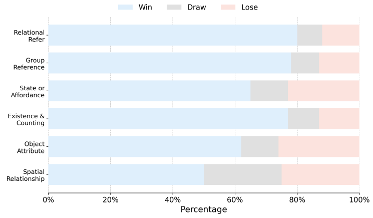

Figure 5: **GPT-Score evaluation.** GPT4Scene holds an advantage on object-level tasks than Chat-scene.

multi-frame input is crucial for achieving the best results. For tasks like 3D QA, a more balanced configuration can be used to optimize for efficiency without a significant loss in performance.

3.4 Ealuation on Spatial Intelligence: VSIBench

We have completed scene understanding and conducted tests on spatial reasoning. Figure 3presents a visual analysis of the GPT4Scene framework’s performance on the VSIBench, a benchmark designed specifically for evaluating spatial intelligence. The primary goal of this evaluation is to validate how effectively GPT4Scene enhances the spatial reasoning capabilities of Vision Language Models (VLMs). The experiments are conducted across two different datasets, ScanNet (”S”) and ARKitScenes (”NS”), to test the framework’s robustness in various types of 3D environments. The key results visualized in the chart show that models integrated with GPT4Scene consistently outperform their baseline counterparts across both datasets. This superiority is particularly evident in tasks that demand a high degree of spatial awareness, such as judging spatial relationships between objects and understanding the overall layout of a scene. This outcome provides strong evidence for the effectiveness of GPT4Scene’s core design principles. By providing global scene context through BEV images and establishing spatio-temporal consistency with STO-markers, the framework successfully empowers VLMs to overcome their previous limitations, thereby significantly strengthening their cognitive and reasoning abilities within complex 3D spaces.

4 Conclusion

We propose GPT4Scene, a framework enhancing VLMs to understand 3D scenes directly from visual inputs. By reconstructing 3D point clouds for Bird’s Eye View (BEV) images and aligning video frames with spatial-temporal object (STO) markers, we enable global-local scene comprehension. GPT4Scene achieves state-of-the-art 3D QA performance with zero-shot GPT-4o and by fine-tuning a series of smaller VLMs using our ScanAlign dataset. These fine-tuned models even excel with raw video inputs, proving effective 3D understanding. Despite its strengths, GPT4Scene relies on point cloud annotations for marker generation due to benchmark constraints. We aim to address this by creating a benchmark that generates STO-markers from video segmentation. We advances indoor understanding by integrating such fine-tuned models as a downstream task for LVLMs.

REFERENCES

Ahmed Abdelreheem, Kyle Olszewski, Hsin-Ying Lee, Peter Wonka, and Panos Achlioptas. Scanents3d: Exploiting phrase-to-3d-object correspondences for improved visio-linguistic models in 3d scenes. In *WACV*, 2024.

Panos Achlioptas, Ahmed Abdelreheem, Fei Xia, Mohamed Elhoseiny, and Leonidas Guibas. Referit3d: Neural listeners for fine-grained 3d object identification in real-world scenes. In *ECCV*, 2020.

Jean-Baptiste Alayrac, Jeff Donahue, Pauline Luc, Antoine Miech, Iain Barr, Yana Hasson, Karel Lenc, Arthur Mensch, Katherine Millican, Malcolm Reynolds, et al. Flamingo: a visual language model for few-shot learning. In *NeurIPS*, 2022.

Kirolos Ataallah, Xiaoqian Shen, Eslam Abdelrahman, Essam Sleiman, Deyao Zhu, Jian Ding, and Mohamed Elhoseiny. Minigpt4-video: Advancing multimodal llms for video understanding with interleaved visual-textual tokens. *arXiv:2404.03413*, 2024.

Daichi Azuma, Taiki Miyanishi, Shuhei Kurita, and Motoaki Kawanabe. Scanqa: 3d question answering for spatial scene understanding. In *CVPR*, 2022.

Eslam Bakr, Yasmeen Alsaedy, and Mohamed Elhoseiny. Look around and refer: 2d synthetic semantics knowledge distillation for 3d visual grounding. In *NeurIPS*, 2022.

Gilad Baruch, Zhuoyuan Chen, Afshin Dehghan, Tal Dimry, Yuri Feigin, Peter Fu, Thomas Gebauer, Brandon Joffe, Daniel Kurz, Arik Schwartz, et al. Arkitscenes: A diverse real-world dataset for 3d indoor scene understanding using mobile rgb-d data. In *NeurIPS*, 2021.

Daigang Cai, Lichen Zhao, Jing Zhang, Lu Sheng, and Dong Xu. 3djcg: A unified framework for joint dense captioning and visual grounding on 3d point clouds. In *CVPR*, 2022.

Keshigeyan Chandrasegaran, Agrim Gupta, Lea M. Hadzic, Taran Kota, Jimming He, Cristóbal Eyzaguirre, Zane Durante, Manling Li, Jiajun Wu, and Li Fei-Fei. Hourvideo: 1-hour video-language understanding. *arXiv:2411.04998*, 2024.

Angel Chang, Angela Dai, Thomas Funkhouser, Maciej Halber, Matthias Niessner, Manolis Savva, Shuran Song, Andy Zeng, and Yinda Zhang. Matterport3d: Learning from rgb-d data in indoor environments. In *3DV*, 2017.

Soravit Changpinyo, Piyush Sharma, Nan Ding, and Radu Soricut. Conceptual 12m: Pushing web-scale image-text pre-training to recognize long-tail visual concepts. In *CVPR*, 2021.

Dave Zhenyu Chen, Angel X Chang, and Matthias Nießner. Scanrefer: 3d object localization in rgb-d scans using natural language. In *ECCV*, 2020.

Dave Zhenyu Chen, Qirui Wu, Matthias Nießner, and Angel X Chang. D3net: a speaker-listener architecture for semi-supervised dense captioning and visual grounding in rgb-d scans. In *ECCV*, 2022a.

Jing Chen, Wenhao Luo, Xizhou Wei, Lin Ma, and Wei Zhang. Ham: Hierarchical attention model with high performance for 3d visual grounding. *arXiv:2210.12513*, 2022b.

Jun Chen, Deyao Zhu, Xiaoqian Shen, Xiang Li, Zechun Liu, Pengchuan Zhang, Raghuraman Krishnamoorthi, Vikas Chandra, Yunyang Xiong, and Mohamed Elhoseiny. Minigpt-v2: large language model as a unified interface for vision-language multi-task learning. *arXiv:2310.09478*, 2023a.

Lin Chen, Jinsong Li, Xiaoyi Dong, Pan Zhang, Yuhang Zang, Zehui Chen, Haodong Duan, Jiaqi Wang, Yu Qiao, Dahua Lin, et al. Are we on the right way for evaluating large vision-language models? In *NeurIPS*, 2024a.

Shizhe Chen, Pierre-Louis Guhur, Makarand Tapaswi, Cordelia Schmid, and Ivan Laptev. Language conditioned spatial relation reasoning for 3d object grounding. In *NeurIPS*, 2022c.

Shizhe Chen, Pierre-Louis Guhur, Makarand Tapaswi, Cordelia Schmid, and Ivan Laptev. Language conditioned spatial relation reasoning for 3d object grounding. In *NeurIPS*, 2022d.

Sijin Chen, Hongyuan Zhu, Xin Chen, Yinjie Lei, Gang Yu, and Tao Chen. End-to-end 3d dense captioning with vote2cap-detr. In *CVPR*, 2023b.

Sijin Chen, Xin Chen, Chi Zhang, Mingsheng Li, Gang Yu, Hao Fei, Hongyuan Zhu, Jiayuan Fan, and Tao Chen. Ll3da: Visual interactive instruction tuning for omni-3d understanding reasoning and planning. In *CVPR*, 2024b.

Yilun Chen, Shuai Yang, Haifeng Huang, Tai Wang, Ruiyuan Lyu, Runsen Xu, Dahua Lin, and Jiangmiao Pang. Grounded 3d-llm with referent tokens. *arXiv:2405.10370*, 2024c.

Zhe Chen, Jiannan Wu, Wenhai Wang, Weijie Su, Guo Chen, Sen Xing, Muyan Zhong, Qinglong Zhang, Xizhou Zhu, Lewei Lu, Bin Li, Ping Luo, Tong Lu, Yu Qiao, and Jifeng Dai. Internvl: Scaling up vision foundation models and aligning for generic visual-linguistic tasks. *arXiv:2312.14238*, 2023c.

Zhenyu Chen, Ali Gholami, Matthias Nießner, and Angel X Chang. Scan2cap: Context-aware dense captioning in rgb-d scans. In *CVPR*, 2021.

Zesen Cheng, Sicong Leng, Hang Zhang, Yifei Xin, Xin Li, Guanzheng Chen, Yongxin Zhu, Wenqi Zhang, Ziyang Luo, Deli Zhao, et al. Videollama 2: Advancing spatial-temporal modeling and audio understanding in video-llms. *arXiv:2406.07476*, 2024.

Angela Dai, Angel X. Chang, Manolis Savva, Maciej Halber, Thomas Funkhouser, and Matthias Nießner. Scannet: Richly-annotated 3d reconstructions of indoor scenes. In *CVPR*, 2017a.

Angela Dai, Matthias Nießner, Michael Zollöfer, Shahram Izadi, and Christian Theobalt. Bundlefusion: Real-time globally consistent 3d reconstruction using on-the-fly surface re-integration. *TOG*, 2017b.

Wenliang Dai, Junnan Li, Dongxu Li, Anthony Meng Huat Tiong, Junqi Zhao, Weisheng Wang, Boyang Li, Pascale Fung, and Steven Hoi. Instructblip: Towards general-purpose vision-language models with instruction tuning. *arXiv:2305.06500*, 2023.

Matt Deitke, Eli VanderBilt, Alvaro Herrasti, Luca Weihs, Kiana Ehsani, Jordi Salvador, Winson Han, Eric Kolve, Aniruddha Kembhavi, and Roozbeh Mottaghi. Procthor: Large-scale embodied ai using procedural generation. In *NeurIPS*, 2022.

Runyu Ding, Jihan Yang, Chuhui Xue, Wenqing Zhang, Song Bai, and Xiaojuan Qi. Pla: Language-driven open-vocabulary 3d scene understanding. In *CVPR*, 2023.

Xiaoyi Dong, Pan Zhang, Yuhang Zang, Yuhang Cao, Bin Wang, Linke Ouyang, Xilin Wei, Songyang Zhang, Haodong Duan, Maosong Cao, Wenwei Zhang, Yining Li, Hang Yan, Yang Gao, Xinyue Zhang, Wei Li, Jingwen Li, Kai Chen, Conghui He, Xingcheng Zhang, Yu Qiao, Dahua Lin, and Jiaqi Wang. Internlm-xcomposer2: Mastering free-form text-image composition and comprehension in vision-language large model. *arXiv:2401.16420*, 2024.

Chaoyou Fu, Yuhan Dai, Yondong Luo, Lei Li, Shuhuai Ren, Renrui Zhang, Zihan Wang, Chenyu Zhou, Yunhang Shen, Mengdan Zhang, et al. Video-mme: The first-ever comprehensive evaluation benchmark of multi-modal llms in video analysis. *arXiv:2405.21075*, 2024a.

Rao Fu, Jingyu Liu, Xilun Chen, Yixin Nie, and Wenhan Xiong. Scene-llm: Extending language model for 3d visual understanding and reasoning. *arXiv:2403.11401*, 2024b.

Ziyu Guo, Renrui Zhang, Xiangyang Zhu, Yiwen Tang, Xianzheng Ma, Jiaming Han, Kexin Chen, Peng Gao, Xianzhi Li, Hongsheng Li, and Pheng-Ann Heng. Point-bind & point-llm: Aligning point cloud with multi-modality for 3d understanding, generation, and instruction following. *arXiv:2309.00615*, 2023a.

Zoey Guo, Yiwen Tang, Ray Zhang, Dong Wang, Zhigang Wang, Bin Zhao, and Xuelong Li. Viewrefer: Grasp the multi-view knowledge for 3d visual grounding. In *ICCV*, 2023b.

Huy Ha and Shuran Song. Semantic abstraction: Open-world 3d scene understanding from 2d vision-language models. In *CoRL*, 2022.

Dailan He, Yusheng Zhao, Junyu Luo, Tianrui Hui, Shaofei Huang, Aixi Zhang, and Si Liu. Transrefer3d: Entity-and-relation aware transformer for fine-grained 3d visual grounding. In *ACMMM*, 2021.

Deepti Hegde, Jeya Maria Jose Valanarasu, and Vishal Patel. Clip goes 3d: Leveraging prompt tuning for language grounded 3d recognition. In *ICCV*, 2023.

Yining Hong, Haoyu Zhen, Peihao Chen, Shuhong Zheng, Yilun Du, Zhenfang Chen, and Chuang Gan. 3d-llm: Injecting the 3d world into large language models. In *NeurIPS*, 2023.

Haifeng Huang, Zehan Wang, Rongjie Huang, Luping Liu, Xize Cheng, Yang Zhao, Tao Jin, and Zhou Zhao. Chat-3d v2: Bridging 3d scene and large language models with object identifiers. *arXiv:2312.08168*, 2023a.

Haifeng Huang, Yilun Chen, Zehan Wang, Rongjie Huang, Runsen Xu, Tai Wang, Luping Liu, Xize Cheng, Yang Zhao, Jiangmiao Pang, et al. Chat-scene: Bridging 3d scene and large language models with object identifiers. In *NeurIPS*, 2024a.

Jiangyong Huang, Silong Yong, Xiaojian Ma, Xiongkun Linghu, Puhao Li, Yan Wang, Qing Li, Song-Chun Zhu, Baoxiong Jia, and Siyuan Huang. An embodied generalist agent in 3d world. *arXiv:2311.12871*, 2023b.

Pao-Hsiang Huang, Hsin-Hsi Lee, Hwann-Tzong Chen, and Tyng-Luh Liu. Text-guided graph neural networks for referring 3d instance segmentation. In *AAAI*, 2021.

Shaohan Huang, Li Dong, Wenhui Wang, Yaru Hao, Saksham Singhal, Shuming Ma, Tengchao Lv, Lei Cui, Owais Khan Mohammed, Barun Patra, et al. Language is not all you need: Aligning perception with language models. In *NeurIPS*, 2024b.

Shijia Huang, Yilun Chen, Jiaya Jia, and Liwei Wang. Multi-view transformer for 3d visual grounding. In *CVPR*, 2022a.

Shijia Huang, Yilun Chen, Jiaya Jia, and Liwei Wang. Multi-view transformer for 3d visual grounding. In *CVPR*, 2022b.

Ayush Jain, Nikolaos Gkanatsios, Ishita Mediratta, and Katerina Fragkiadaki. Bottom up top down detection transformers for language grounding in images and point clouds. In *ECCV*, 2022.

Baoxiong Jia, Yixin Chen, Huangyue Yu, Yan Wang, Xuesong Niu, Tengyu Liu, Qing Li, and Siyuan Huang. Sceneverse: Scaling 3d vision-language learning for grounded scene understanding. In *ECCV*, 2024.

Li Jiang, Hengshuang Zhao, Shaoshuai Shi, Shu Liu, Chi-Wing Fu, and Jiaya Jia. Pointgroup: Dual-set point grouping for 3d instance segmentation. In *CVPR*, 2020.

Zhao Jin, Munawar Hayat, Yuwei Yang, Yulan Guo, and Yinjie Lei. Context-aware alignment and mutual masking for 3d-language pre-training. In *CVPR*, 2023.

Weitai Kang, Haifeng Huang, Yuzhang Shang, Mubarak Shah, and Yan Yan. Robin3d: Improving 3d large language model via robust instruction tuning. *arXiv:2410.00255*, 2024a.

Weitai Kang, Mengxue Qu, Jyoti Kini, Yunchao Wei, Mubarak Shah, and Yan Yan. Intent3d: 3d object detection in rgb-d scans based on human intention. *arXiv:2405.18295*, 2024b.

Mukul Khanna, Yongsen Mao, Hanxiao Jiang, Sanjay Haresh, Brennan Shacklett, Dhruv Batra, Alexander Clegg, Eric Undersander, Angel X Chang, and Manolis Savva. Habitat synthetic scenes dataset (hssd-200): An analysis of 3d scene scale and realism tradeoffs for objectgoal navigation. In *CVPR*, 2024.

Xin Lai, Zhuotao Tian, Yukang Chen, Yanwei Li, Yuhui Yuan, Shu Liu, and Jiaya Jia. Lisa: Reasoning segmentation via large language model. In *CVPR*, 2024.

Bo Li, Yuanhan Zhang, Dong Guo, Renrui Zhang, Feng Li, Hao Zhang, Kaichen Zhang, Yanwei Li, Ziwei Liu, and Chunyuan Li. Llava-onevision: Easy visual task transfer. *arXiv:2408.03326*, 2024.

Chengzu Li, Wenshan Wu, Huanyu Zhang, Yan Xia, Shaoguang Mao, Li Dong, Ivan Vulić, and Furu Wei. Imagine while reasoning in space: Multimodal visualization-of-thought. *arXiv:2501.07542*, 2025.

Junnan Li, Dongxu Li, Caiming Xiong, and Steven Hoi. Blip: Bootstrapping language-image pre-training for unified vision-language understanding and generation. In *ICML*, 2022.

Junnan Li, Dongxu Li, Silvio Savarese, and Steven Hoi. Blip-2: Bootstrapping language-image pre-training with frozen image encoders and large language models. *arXiv:2301.12597*, 2023a.

Kunchang Li, Yali Wang, Yinan He, Yizhuo Li, Yi Wang, Yi Liu, Zun Wang, Jilan Xu, Guo Chen, Ping Luo, Limin Wang, and Yu Qiao. Mvbench: A comprehensive multi-modal video understanding benchmark. *arXiv:2311.17005*, 2023b.

Yanwei Li, Chengyao Wang, and Jiaya Jia. Llama-vid: An image is worth 2 tokens in large language models. *arXiv:2311.17043*, 2023c.

Benlin Liu, Yuhao Dong, Yiqin Wang, Yongming Rao, Yansong Tang, Wei-Chiu Ma, and Ranjay Krishna. Coarse correspondence elicit 3d spacetime understanding in multimodal language model. *arXiv:2408.00754*, 2024a.

Haotian Liu, Chunyuan Li, Qingyang Wu, and Yong Jae Lee. Visual instruction tuning. In *NeurIPS*, 2023.

Haotian Liu, Chunyuan Li, Yuheng Li, and Yong Jae Lee. Improved baselines with visual instruction tuning. In *CVPR*, 2024b.

Haotian Liu, Chunyuan Li, Yuheng Li, Bo Li, Yuanhan Zhang, Sheng Shen, and Yong Jae Lee. Llava-next: Improved reasoning, ocr, and world knowledge, 2024c. URL https://llava-vl.github.io/blog/2024-01-30-llava-next.

Junyu Luo, Jiahui Fu, Xianghao Kong, Chen Gao, Haibing Ren, Hao Shen, Huaxia Xia, and Si Liu. 3d-sps: Single-stage 3d visual grounding via referred point progressive selection. In *CVPR*, 2022.

Ruipu Luo, Ziwang Zhao, Min Yang, Junwei Dong, Minghui Qiu, Pengcheng Lu, Tao Wang, and Zhongyu Wei. Valley: Video assistant with large language model enhanced ability. *arXiv:2306.07207*, 2023.

Xiaojian Ma, Silong Yong, Zilong Zheng, Qing Li, Yitao Liang, Song-Chun Zhu, and Siyuan Huang. Sqa3d: Situated question answering in 3d scenes. In *ICLR*, 2023.

Muhammad Maaz, Hanoona Rasheed, Salman Khan, and Fahad Shahbaz Khan. Video-chatgpt: Towards detailed video understanding via large vision and language models. *arXiv:2306.05424*, 2023.

Yunze Man, Shuhong Zheng, Zhipeng Bao, Martial Hebert, Liang-Yan Gui, and Yu-Xiong Wang. Lexicon3d: Probing visual foundation models for complex 3d scene understanding. In *NeurIPS*, 2024.

Yongsen Mao, Yiming Zhang, Hanxiao Jiang, Angel Chang, and Manolis Savva. Multiscan: Scalable rgbd scanning for 3d environments with articulated objects. In *NeurIPS*, 2022.

Ishan Misra, Rohit Girdhar, and Armand Joulin. An end-to-end transformer model for 3d object detection. In *ICCV*, 2021.

OpenAI. Gpt-4 technical report. *arXiv:2303.08774*, 2023.

OpenAI. Gpt-4o: A large language model by openai. https://openai.com/research/gpt-4o, 2024.

Songyou Peng, Kyle Genova, Chiyu Jiang, Andrea Tagliasacchi, Marc Pollefeys, Thomas Funkhouser, et al. Openscene: 3d scene understanding with open vocabularies. In *CVPR*, 2023a.

Zhiliang Peng, Wenhui Wang, Li Dong, Yaru Hao, Shaohan Huang, Shuming Ma, and Furu Wei. Kosmos-2: Grounding multimodal large language models to the world. *arXiv:2306.14824*, 2023b.

Charles R Qi, Or Litany, Kaiming He, and Leonidas J Guibas. Deep hough voting for 3d object detection in point clouds. In *ICCV*, 2019.

Zekun Qi, Runpei Dong, Shaochen Zhang, Haoran Geng, Chunrui Han, Zheng Ge, Li Yi, and Kaisheng Ma. Shapellm: Universal 3d object understanding for embodied interaction. In *ECCV*, 2024a.

Zhangyang Qi, Ye Fang, Zeyi Sun, Xiaoyang Wu, Tong Wu, Jiaqi Wang, Dahua Lin, and Hengshuang Zhao. Gpt4point: A unified framework for point-language understanding and generation. In *CVPR*, 2024b.

Alec Radford, Jong Wook Kim, Chris Hallacy, Aditya Ramesh, Gabriel Goh, Sandhini Agarwal, Girish Sastry, Amanda Askell, Pamela Mishkin, Jack Clark, et al. Learning transferable visual models from natural language supervision. In *ICML*, 2021.

Santhosh K Ramakrishnan, Aaron Gokaslan, Erik Wijmans, Oleksandr Maksymets, Alex Clegg, John Turner, Eric Undersander, Wojciech Galuba, Andrew Westbury, Angel X Chang, et al. Habitat-matterport 3d dataset (hm3d): 1000 large-scale 3d environments for embodied ai. In *NeurIPS*, 2021.

Hanoona Rasheed, Muhammad Maaz, Sahal Shaji, Abdelrahman Shaker, Salman Khan, Hisham Cholakkal, Rao M Anwer, Erix Xing, Ming-Hsuan Yang, and Fahad S Khan. Glamm: Pixel grounding large multimodal model. *arXiv:2311.03356*, 2023.

Shuhuai Ren, Linli Yao, Shicheng Li, Xu Sun, and Lu Hou. Timechat: A time-sensitive multimodal large language model for long video understanding. *arXiv:2312.02051*, 2023.

Christoph Schuhmann, Romain Beaumont, Richard Vencu, Cade Gordon, Ross Wightman, Mehdi Cherti, Theo Coombes, Aarush Katta, Clayton Mullis, Mitchell Wortsman, et al. Laion-5b: An open large-scale dataset for training next generation image-text models. In *NeurIPS*, 2022.

Jonas Schult, Francis Engelmann, Alexander Hermans, Or Litany, Siyu Tang, and Bastian Leibe. Mask3d: Mask transformer for 3d semantic instance segmentation. In *ICRA*, 2023.

Enxin Song, Wenhao Chai, Guanhong Wang, Yucheng Zhang, Haoyang Zhou, Feiyang Wu, Xun Guo, Tian Ye, Yan Lu, Jenq-Neng Hwang, et al. Moviechat: From dense token to sparse memory for long video understanding. *arXiv:2307.16449*, 2023.

Julian Straub, Thomas Whelan, Lingni Ma, Yufan Chen, Erik Wijmans, Simon Green, Jakob J Engel, Raul Mur-Artal, Carl Ren, Shobhit Verma, et al. The replica dataset: A digital replica of indoor spaces. *arXiv:1906.05797*, 2019.

Quan Sun, Qiying Yu, Yufeng Cui, Fan Zhang, Xiaosong Zhang, Yueze Wang, Hongcheng Gao, Jingjing Liu, Tiejun Huang, and Xinlong Wang. Emu: Generative pretraining in multimodality. In *ICLR*, 2023.

Ayça Takmaz, Elisabetta Fedele, Robert W Sumner, Marc Pollefeys, Federico Tombari, and Francis Engelmann. Openmask3d: Open-vocabulary 3d instance segmentation. In *NeurIPS*, 2023.

Gemini Team. Gemini 1.5: Unlocking multimodal understanding across millions of tokens of context. *arXiv:2403.05530*, 2024a.

Gemma Team and Google DeepMind. Gemma 2: Improving open language models at a practical size. *arXiv:2408.00118*, 2024.

InternLM Team. Internlm2 technical report. *arXiv:2403.17297*, 2024b.

Llama Team. The llama 3 herd of models. *arXiv:2407.21783*, 2024c.

Qwen Team. Qwen2.5 technical report. *arXiv:2412.15115*, 2024d.

Ozan Unal, Christos Sakaridis, Suman Saha, and Luc Van Gool. Four ways to improve verbo-visual fusion for dense 3d visual grounding. In *ECCV*, 2024.

Thang Vu, Kookhoi Kim, Tung M Luu, Thanh Nguyen, and Chang D Yoo. Softgroup for 3d instance segmentation on point clouds. In *CVPR*, 2022.

Johanna Wald, Armen Avetisyan, Nassir Navab, Federico Tombari, and Matthias Nießner. Rio: 3d object instance re-localization in changing indoor environments. In *ICCV*, 2019.

Haochen Wang, Yucheng Zhao, Tiancai Wang, Haoqiang Fan, Xiangyu Zhang, and Zhaoxiang Zhang. Ross3d: Reconstructive visual instruction tuning with 3d-awareness, 2025. URL https://arxiv.org/abs/2504.01901.

Peng Wang, Shuai Bai, Sinan Tan, Shijie Wang, Zhihao Fan, Jinze Bai, Keqin Chen, Xuejing Liu, Jialin Wang, Wenbin Ge, Yang Fan, Kai Dang, Mengfei Du, Xuancheng Ren, Rui Men, Dayiheng Liu, Chang Zhou, Jingren Zhou, and Junyang Lin. Qwen2-vl: Enhancing vision-language model's perception of the world at any resolution. *arXiv:2409.12191*, 2024a.

Tai Wang, Xiaohan Mao, Chenming Zhu, Runsen Xu, Ruiyuan Lyu, Peisen Li, Xiao Chen, Wenwei Zhang, Kai Chen, Tianfan Xue, Xihui Liu, Cewu Lu, Dahua Lin, and Jiangmiao Pang. Embodiedscan: A holistic multi-modal 3d perception suite towards embodied ai. In *CVPR*, 2024b.

Weihan Wang, Qingsong Lv, Wenmeng Yu, Wenyi Hong, Ji Qi, Yan Wang, Junhui Ji, Zhuoyi Yang, Lei Zhao, Xixuan Song, et al. Cogvlm: Visual expert for pretrained language models. *arXiv:2311.03079*, 2023a.

Zehan Wang, Haifeng Huang, Yang Zhao, Linjun Li, Xize Cheng, Yichen Zhu, Aoxiong Yin, and Zhou Zhao. 3drp-net: 3d relative position-aware network for 3d visual grounding. In *EMNLP*, 2023b.

Zehan Wang, Haifeng Huang, Yang Zhao, Ziang Zhang, and Zhou Zhao. Chat-3d: Data-efficiently tuning large language model for universal dialogue of 3d scenes. *arXiv:2308.08769*, 2023c.

Ting-Yao Wu, Shih-Yang Huang, and Yung-Chen Francis Wang. Dora: 3d visual grounding with order-aware referring. *arXiv:2403.16539*, 2024a.

Xiaoyang Wu, Li Jiang, Peng-Shuai Wang, Zhijian Liu, Xihui Liu, Yu Qiao, Wanli Ouyang, Tong He, and Hengshuang Zhao. Point transformer v3: Simpler, faster, stronger. In *CVPR*, 2024b.

Yanmin Wu, Xinhua Cheng, Renrui Zhang, Zesen Cheng, and Jian Zhang. Eda: Explicit text-decoupling and dense alignment for 3d visual grounding. In *CVPR*, 2023.

xAI, 2024. URL https://huggingface.co/datasets/xai-org/RealworldQA/tree/main.

Runsen Xu, Zhiwei Huang, Tai Wang, Yilun Chen, Jiangmiao Pang, and Dahua Lin. Vlm-grounder: A vlm agent for zero-shot 3d visual grounding. In *CoRL*, 2024a.

Runsen Xu, Xiaolong Wang, Tai Wang, Yilun Chen, Jiangmiao Pang, and Dahua Lin. Pointllm: Empowering large language models to understand point clouds. In *ECCV*, 2024b.

Le Xue, Mingfei Gao, Chen Xing, Roberto Martín-Martín, Jiajun Wu, Caiming Xiong, Ran Xu, Juan Carlos Niebles, and Silvio Savarese. Ulip: Learning a unified representation of language, images, and point clouds for 3d understanding. In *CVPR*, 2023.

Jihan Yang, Runyu Ding, Zhe Wang, and Xiaojuan Qi. Regionplc: Regional point-language contrastive learning for open-world 3d scene understanding. *arXiv:2304.00962*, 2023.

Jihan Yang, Shusheng Yang, Anjali Gupta, Rilyn Han, Li Fei-Fei, and Saining Xie. Thinking in Space: How Multimodal Large Language Models See, Remember and Recall Spaces. In *CVPR*, 2025.

Zhengyuan Yang, Songyang Zhang, Liwei Wang, and Jiebo Luo. Sat: 2d semantics assisted training for 3d visual grounding. In *ICCV*, 2021.

Shuquan Ye, Dongdong Chen, Songfang Han, and Jing Liao. 3d question answering. *TVCG*, 2022.

Zhihao Yuan, Xu Yan, Yinghong Liao, Ruimao Zhang, Zhen Li, and Shuguang Cui. Instancerefer: Cooperative holistic understanding for visual grounding on point clouds through instance multi-level contextual referring. In *ICCV*, 2021.

Zhihao Yuan, Xu Yan, Yinghong Liao, Yao Guo, Guanbin Li, Shuguang Cui, and Zhen Li. X-trans2cap: Cross-modal knowledge transfer using transformer for 3d dense captioning. In *CVPR*, 2022.

Yuanhan Zhang et. al Yuan Liu, Haodong Duan. Mmbench: Is your multi-modal model an all-around player? *arXiv:2307.06281*, 2023.

Xiaoyang Wu et.al Yunhan Yang. Sam3d: Segment anything in 3d scenes. In *ICCV Workshop*, 2023.

Hang Zhang, Xin Li, and Lidong Bing. Video-llama: An instruction-tuned audio-visual language model for video understanding. *arXiv:2306.02858*, 2023a.

Renrui Zhang, Ziyu Guo, Wei Zhang, Kunchang Li, Xupeng Miao, Bin Cui, Yu Qiao, Peng Gao, and Hongsheng Li. Pointclip: Point cloud understanding by clip. In *CVPR*, 2022.

Renrui Zhang, Liuhui Wang, Yu Qiao, Peng Gao, and Hongsheng Li. Learning 3d representations from 2d pre-trained models via image-to-point masked autoencoders. In *CVPR*, 2023b.

Sha Zhang, Di Huang, Jiajun Deng, Shixiang Tang, Wanli Ouyang, Tong He, and Yanyong Zhang. Agent3d-zero: An agent for zero-shot 3d understanding. In *ECCV*, 2024.

Yiming Zhang, ZeMing Gong, and Angel X Chang. Multi3drefer: Grounding text description to multiple 3d objects. In *ICCV*, 2023c.

Lichen Zhao, Daigang Cai, Lu Sheng, and Dong Xu. 3dvg-transformer: Relation modeling for visual grounding on point clouds. In *ICCV*, 2021.

Duo Zheng, Shijia Huang, and Liwei Wang. Video-3d llm: Learning position-aware video representation for 3d scene understanding. In *CVPR*, 2025.

Jia Zheng, Junfei Zhang, Jing Li, Rui Tang, Shenghua Gao, and Zihan Zhou. Structured3d: A large photo-realistic dataset for structured 3d modeling. In *ECCV*, 2020.

Chenming Zhu, Tai Wang, Wenwei Zhang, Jiangmiao Pang, and Xihui Liu. Llava-3d: A simple yet effective pathway to empowering lmms with 3d-awareness. *arXiv:2409.18125*, 2024a.

Deyao Zhu, Jun Chen, Xiaoqian Shen, Xiang Li, and Mohamed Elhoseiny. Minigpt-4: Enhancing vision-language understanding with advanced large language models. *arXiv:2304.10592*, 2023a.

Ziyu Zhu, Xiaojian Ma, Yixin Chen, Zhidong Deng, Siyuan Huang, and Qing Li. 3d-vista: Pre-trained transformer for 3d vision and text alignment. In *ICCV*, 2023b.

Ziyu Zhu, Zhuofan Zhang, Xiaojian Ma, Xuesong Niu, Yixin Chen, Baoxiong Jia, Zhidong Deng, Siyuan Huang, and Qing Li. Unifying 3d vision-language understanding via promptable queries. In *ECCV*, 2024b.

A LLM Usage Statement

During the preparation of this manuscript, we utilized a Large Language Model (LLM) as an assistive tool. The primary role of the LLM was for language polishing, which included improving grammar, enhancing the clarity and fluency of the text, and ensuring consistent use of technical terminology. All core research ideas, methodologies, experimental designs, results, and conclusions were conceived and formulated exclusively by the human authors. The LLM did not contribute to any of the substantive scientific aspects of this work. We have carefully reviewed and edited all text modified with the assistance of the LLM and take full responsibility for the final content of.

B Prompts of Closed-source VLMs

Here, we present the prompts used by GPT4Scene in the closed-source VLMs (GPT-4o), as illustrated in Figure 6. The process begins with a general **system prompt**, which outlines the overview of two images provided as input. The first image is a stitched 2D view captured from a video, with dimensions of 2×4. The second image represents a **BEV** (Bird's Eye View). Subsequently, we perform evaluations across various tasks and benchmarks, with each benchmark associated with a specific prompt. We take the 3D question-answering task on **ScanQA** as an example. The benchmark prompt consists of three parts:

1. **Important Guidelines:** It clarifies that while we provide object IDs for reference, they cannot be directly used when answering questions. Additionally, it specifies adapting the response style to match that of ScanQA. Since ScanQA's responses are typically short single words, we aim to keep the answers concise within the benchmark prompt, targeting 1-5 words.
2. **Answer Format:** In this part, we use a standardized regularized format to structure the answers, which helps improve accuracy when addressing questions.
3. **Examples:** we include two example cases.

Our **zero-shot prompting process** is illustrated in the bottom-left corner Figure 6. The system prompt and ScanQA prompt are used as the system message. In the user message, we input the stitched image and BEV image. Finally, the query message includes the question. The responses generated through this process require further refinement, as depicted in the bottom-right corner of Figure 6. First, we remove the regularized formatting from the answers. Next, we clean the answers by addressing singular/plural forms and case sensitivity. This final step ensures that we obtain the refined answers.

C 2D Multi-modal Benchmark

We tested the fine-tuned *Qwen2-VL-7B (GPT4Scene)* model on 2D image and video multimodal large models. Table 10 shows the results of MVBench. As we can see, our model shows improvement for the object and action metrics, indicating that the model fine-tuned with ScanAlign is better at handling spatial variations and the information of objects in the scene. Table 11 presents the results on other benchmarks, where we can observe that after our fine-tuning, the model's ability to understand images and videos did not decline significantly. It demonstrates the effectiveness of ScanAlign.

D Qualitative Results

Figures 7 to 10 present our qualitative results obtained from Qwen2-VL after fine-tuning on ScanAlign. Figures 7 and 8 demonstrate 3D question answering performance using only unannotated video inputs as context. Our observations indicate the model's capability to effectively address queries from both ScanQA Azuma et al. (2022) and SQA3D Ma et al. (2023) benchmarks. Meanwhile, Figures 9 and 10 exhibit the model's competence in 3D dense captioning and 3D visual grounding tasks requiring annotated inputs. These outcomes substantiate that our framework can generate precise responses through visual information processing alone, without dependency

Task type	Model	
	Qwen2-VL	Ours
Action Sequence	85.5	82.0
Action Prediction	69.5	**70.5**
Action Antonym	83.0	**86.0**
Fine-grained Action	51.5	51.5
Unexpected Action	82.0	78.0
Object Existence	87.5	**88.5**
Object Interaction	82.0	81.5
Object Shuffle	41.0	**45.0**
Moving Direction	42.0	40.0
Action Localization	65.0	**66.5**
Scene Transition	93.5	**94.0**
Action Count	47.5	43.5
Moving Count	69.5	71.5
Moving Attribute	90.0	88.5
State Change	48.0	**49.0**
Fine-grained Pose	63.0	63.5
Character Order	74.5	71.0
Egocentric Navigation	39.5	**41.5**
Episodic Reasoning	47.0	47.0
Counterfactual Inference	62.5	**65.5**
Avg	**66.2**	**66.225**

Table 10: **The result of MVBench Li et al. (2023b).** After fine-tuning with ScanAlign in GPT4Scene, our model shows improved 2D understanding, particularly in object and action metrics.

Benchmark	Model	
	Qwen2-VL	Ours
MMBench-EN$_{val}$ Yuan Liu (2023)	82.4	81.2
MMBench-CN$_{val}$ Yuan Liu (2023)	81.7	79.9
MMStar Chen et al. (2024a)	60.7	57.6
RealWorldQA xAI (2024)	70.1	68.5
Video-MME Fu et al. (2024a)	59.8	58.4

Table 11: **The result of 2D Multi-modal Benchmark.** After fine-tuning with ScanAlign in GPT4Scene, our model's 2D understanding capabilities did not decline.

on 3D point cloud inputs. Here we emphasize that post-training with the GPT4Scene framework, the model achieves accurate QA performance using only pure video input, thereby demonstrating GPT4Scene's effectiveness in enhancing visual comprehension capabilities.

E Full Quantitive Results

Here, we present the complete metrics for all five benchmarks. Table 12 and Table 13 show results for ScanQA Azuma et al. (2022) and SQA3D Ma et al. (2023). Table 14 provides the full results for

Methods	EM-1	BLEU-n Metrics				Language Generation Metrics		
		BLEU-1	BLEU-2	BLEU-3	BLEU-4	ROUGE	METEOR	CIDEr
Task-Specific Model								
ScanQA Azuma et al. (2022)	21.1	30.2	20.4	15.1	10.1	33.3	13.1	64.9
3D-VLP Jin et al. (2023)	21.7	30.5	21.3	16.7	11.2	34.5	13.5	67.0
3D-Vista Zhu et al. (2023b)	–	–	–	–	13.9	35.7	–	–
3D LLM Based Model								
3D-LLM Hong et al. (2023)	20.5	39.3	25.2	18.4	12.0	35.7	14.5	69.4
LL3DA Chen et al. (2024b)	–	–	–	–	13.5	37.3	15.9	76.8
LEO Huang et al. (2023b)	24.5	–	–	–	11.5	39.3	16.2	80.0
Scene-LLM Fu et al. (2024b)	27.2	43.6	26.8	19.1	12.0	40.0	16.6	80.0
Chat-scene Huang et al. (2024a)	21.6	43.2	29.1	20.6	14.3	41.6	18.0	87.7
Vision LLM Based Model								
InternVL3-8B (GPT4Scene)	29.5	45.1	30.7	22.7	16.2	47.8	19.5	96.8
Qwen2-VL-7B (GPT4Scene)	28.2	44.4	30.3	22.3	15.5	46.5	18.9	96.3
Qwen2.5-VL-7B (GPT4Scene)	31.2	49.2	38.2	28.3	19.8	50.2	21.1	105.7

Table 12: **Full Evaluation of 3D Question Answering on ScanQA Azuma et al. (2022).**

Methods	Test Set						Avg.(EM-1)	EM-R1
	What	Is	How	Can	Which	Others		
Task-Specific Model								
ClipBERT Ma et al. (2023)	30.2	60.1	38.7	63.3	42.5	42.7	43.3	–
SQA3D Ma et al. (2023)	31.6	63.8	46.0	69.5	43.9	45.3	46.6	–
3D-VisTA Zhu et al. (2023b)	34.8	63.3	45.4	69.8	47.2	48.1	48.5	–
3D LLM Based Model								
PQ3D Zhu et al. (2024b)	37.1	61.3	44.5	60.9	47.0	45.1	47.1	–
LEO Huang et al. (2023b)	–	–	–	–	–	–	50.0	52.4
Scene-LLM Fu et al. (2024b)	40.9	69.1	45.0	**70.8**	47.2	52.3	54.2	–
Chat-scene Huang et al. (2024a)	45.4	67.0	52.0	69.5	49.9	55.0	54.6	57.5
Vision LLM Based Model								
InternVL3-8B (GPT4Scene)	58.0	71.9	53.0	70.8	55.3	62.4	61.9	64.5
Qwen2-VL-7B (GPT4Scene)	55.9	69.9	50.8	68.7	53.3	60.4	59.4	62.4
Qwen2.5-VL-7B (GPT4Scene)	60.1	72.5	55.5	71.8	56.3	64.0	63.5	66.2

Table 13: **Full Evaluation of 3D Question Answering on SQA3D Ma et al. (2023).**

Methods	IoU@0.25				IoU@0.5			
	CIDEr	BLEU-4	METEOR	ROUGE	CIDEr	BLEU-4	METEOR	ROUGE
Task-Specific Model								
Scan2Cap Chen et al. (2021)	56.8	34.2	26.3	55.3	39.1	23.3	22.0	44.5
3DJCG Cai et al. (2022)	64.7	40.2	27.7	59.2	49.5	31.0	24.2	50.8
X-Trans2Cap Yuan et al. (2022)	61.8	35.7	26.6	54.7	43.9	25.1	22.5	45.3
D3Net Chen et al. (2022a)	–	–	–	–	62.6	35.7	25.7	53.9
3D-VLP Jin et al. (2023)	70.7	41.0	28.1	59.7	54.9	32.3	24.8	51.5
Vote2Cap-DETR Chen et al. (2023b)	71.5	39.3	28.3	59.3	62.6	35.7	25.7	53.9
3D-VisTA Zhu et al. (2023b)	71.0	36.5	28.4	57.6	66.9	34.0	27.1	54.3
3D LLM Based Model								
LL3DA Chen et al. (2024b)	74.2	41.4	27.8	59.5	65.2	36.8	26.0	55.1
LEO Huang et al. (2023b)	–	–	–	–	68.4	36.9	27.7	57.8
Chat-scene Huang et al. (2024a)	81.9	38.2	29.0	60.6	77.2	36.3	28.0	58.1
Robin3D Kang et al. (2024a)	–	–	–	–	**87.2**	38.4	–	–
Vision LLM Based Model								
InternVL3-8B (GPT4Scene)	93.5	44.1	29.8	63.1	88.1	41.4	28.7	60.3
Qwen2-VL-7B (GPT4Scene)	91.7	43.1	29.3	61.9	86.3	40.6	28.2	59.3
Qwen2.5-VL-7B (GPT4Scene)	98.2	45.9	31.5	67.9	92.5	44.1	30.1	67.1

Table 14: **Full Evaluation of 3D Dense Caption on Scan2Cap Chen et al. (2021).**

Scan2Cap Chen et al. (2021), while Table 15 and Table 16 present the results for ScanRefer Chen et al. (2020) and Multi3DRef Zhang et al. (2023c). Our model significantly improves across all benchmarks, highlighting that only pure vision language models can understand 3D scenes effectively.

Methods	Unique		Multiple		Overall	
	Acc@0.25	Acc@0.5	Acc@0.25	Acc@0.5	Acc@0.25	Acc@0.5
Task-Specific Model						
ScanRefer Chen et al. (2020)	76.3	53.5	32.7	21.1	41.2	27.4
TGNN Huang et al. (2021)	68.6	56.8	29.8	23.2	37.4	29.7
SAT Yuan et al. (2022)	73.2	50.8	37.6	25.2	44.5	30.1
InstanceRefer Yuan et al. (2021)	75.7	64.7	29.4	23.0	38.4	31.1
3DVG-Transformer Zhao et al. (2021)	81.9	60.6	39.3	28.4	47.6	34.7
MVT Huang et al. (2022a)	77.7	66.4	31.9	25.3	40.8	33.3
3D-SPS Luo et al. (2022)	84.1	66.7	40.3	29.8	48.8	37.0
ViL3DRel Chen et al. (2022d)	81.6	68.6	40.3	30.7	47.9	37.7
3DJCG Cai et al. (2022)	83.5	64.3	41.4	30.8	49.6	37.3
D3Net Chen et al. (2022a)	–	72.0	–	30.1	–	37.9
BUTD-DETR Jain et al. (2022)	84.2	66.3	46.6	35.1	52.2	39.8
HAM Chen et al. (2022b)	79.2	67.9	41.5	34.0	48.8	40.6
3DRP-Net Wang et al. (2023b)	83.1	67.7	42.1	32.0	50.1	38.9
3D-VLP Jin et al. (2023)	84.2	64.6	43.5	33.4	51.4	39.5
EDA Wu et al. (2023)	85.8	68.6	**49.1**	37.6	54.6	42.3
M3DRef-CLIP Zhang et al. (2023c)	85.3	77.2	43.8	36.8	51.9	44.7
3D-VisTA Zhu et al. (2023b)	81.6	75.1	43.7	39.1	50.6	45.8
ConcreteNet Unal et al. (2024)	86.4	82.1	42.4	38.4	50.6	46.5
DOrA Wu et al. (2024a)	–	–	–	–	52.8	44.8
3D LLM Based Model						
Chat-scene Huang et al. (2024a)	89.6	82.5	47.8	42.9	55.5	50.2
Robin3D Kang et al. (2024a)	–	–	–	–	60.8	55.1
Vision LLM Based Model						
InternVL3-8B (GPT4Scene)	90.8	84.5	57.2	51.8	63.4	57.7
Qwen2-VL-7B (GPT4Scene)	90.3	83.7	56.4	50.9	62.6	57.0
Qwen2.5-VL-7B (GPT4Scene)	91.5	85.8	59.2	53.7	65.6	59.5

Table 15: **Full Evaluation of 3D Visual Grounding on ScanRefer Chen et al. (2020).**

Methods	ZT w/o D	ZT w/ D	ST w/o D		ST w/ D		MT		ALL	
	F1	F1	F1@0.25	F1@0.5	F1@0.25	F1@0.5	F1@0.25	F1@0.5	F1@0.25	F1@0.5
Task-Specific Model										
3DVG-Trans+ Zhao et al. (2021)	87.1	45.8	–	27.5	–	16.7	–	26.5	–	25.5
D3Net (Grounding) Chen et al. (2022a)	81.6	32.5	–	38.6	–	23.3	–	35.0	–	32.2
3DJCG (Grounding) Cai et al. (2022)	94.1	66.9	–	26.0	–	16.7	–	26.2	–	26.6
M3DRef-CLIP Zhang et al. (2023c)	81.8	39.4	53.5	47.8	34.6	30.6	43.6	37.9	42.8	38.4
3D LLM Based Model										
Chat-scene Huang et al. (2024a)	90.3	62.6	82.9	75.9	49.1	44.5	45.7	41.1	57.1	52.4
Vision LLM Based Model										
InternVL3-8B (GPT4Scene)	97.6	85.1	85.5	78.3	60.8	55.9	49.2	45.3	65.5	60.7
Qwen2-VL-7B (GPT4Scene)	97.4	84.4	85.0	77.7	59.9	55.1	48.6	44.6	64.5	59.8
Qwen2.5-VL-7B (GPT4Scene)	98.0	86.5	86.8	79.9	62.5	57.8	51.0	47.1	67.3	62.8

Table 16: **Full Evaluation of 3D Visual Grounding on Multi3DRef Zhang et al. (2023c).**

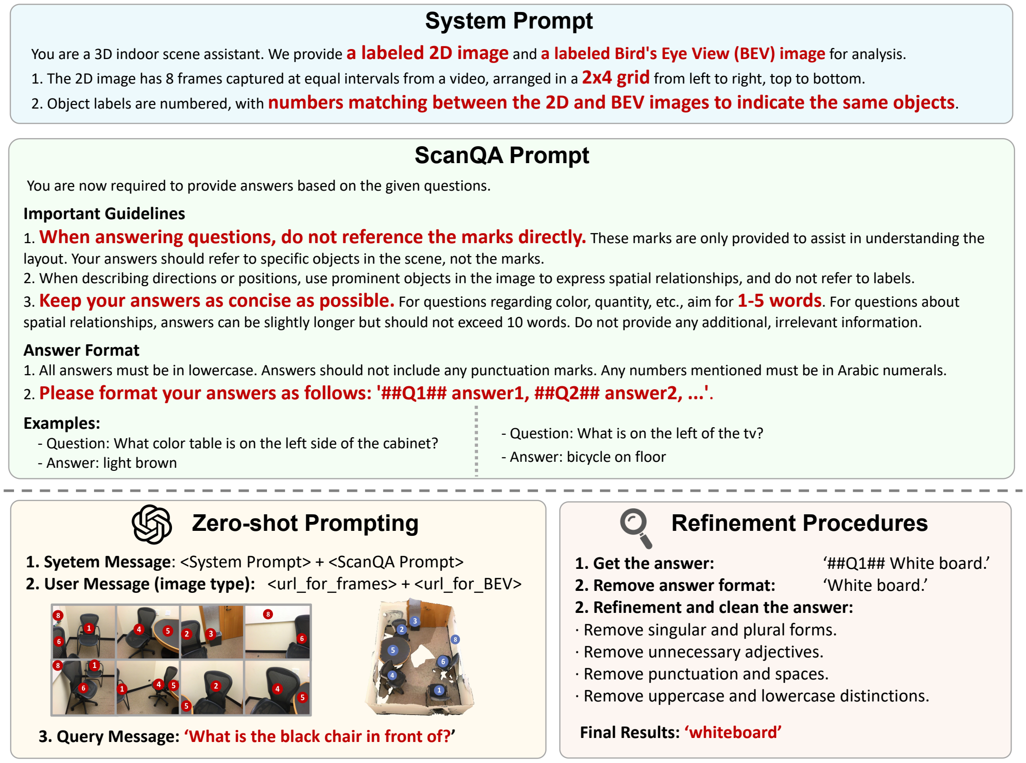

System Prompt

You are a 3D indoor scene assistant. We provide **a labeled 2D image** and **a labeled Bird's Eye View (BEV) image** for analysis.
1. The 2D image has 8 frames captured at equal intervals from a video, arranged in a **2x4 grid** from left to right, top to bottom.
2. Object labels are numbered, with **numbers matching between the 2D and BEV images to indicate the same objects**.

ScanQA Prompt

You are now required to provide answers based on the given questions.

Important Guidelines

1. **When answering questions, do not reference the marks directly.** These marks are only provided to assist in understanding the layout. Your answers should refer to specific objects in the scene, not the marks.
2. When describing directions or positions, use prominent objects in the image to express spatial relationships, and do not refer to labels.
3. **Keep your answers as concise as possible.** For questions regarding color, quantity, etc., aim for **1-5 words**. For questions about spatial relationships, answers can be slightly longer but should not exceed 10 words. Do not provide any additional, irrelevant information.

Answer Format

1. All answers must be in lowercase. Answers should not include any punctuation marks. Any numbers mentioned must be in Arabic numerals.
2. **Please format your answers as follows: '##Q1## answer1, ##Q2## answer2, ...'.**

Examples:
- Question: What color table is on the left side of the cabinet?
- Answer: light brown

- Question: What is on the left of the tv?
- Answer: bicycle on floor

Zero-shot Prompting

1. Syetem Message: <System Prompt> + <ScanQA Prompt>
2. User Message (image type): <url_for_frames> + <url_for_BEV>

3. Query Message: 'What is the black chair in front of?'

Refinement Procedures

1. Get the answer: '##Q1## White board.'
2. Remove answer format: 'White board.'
2. Refinement and clean the answer:
· Remove singular and plural forms.
· Remove unnecessary adjectives.
· Remove punctuation and spaces.
· Remove uppercase and lowercase distinctions.

Final Results: 'whiteboard'

Figure 6: **Prompts of Closed-sourse VLMs.** We show the prompts used for GPT-4o (GPT4Scene), which consist of a system prompt and a benchmark prompt. After generating responses, we further refine them.

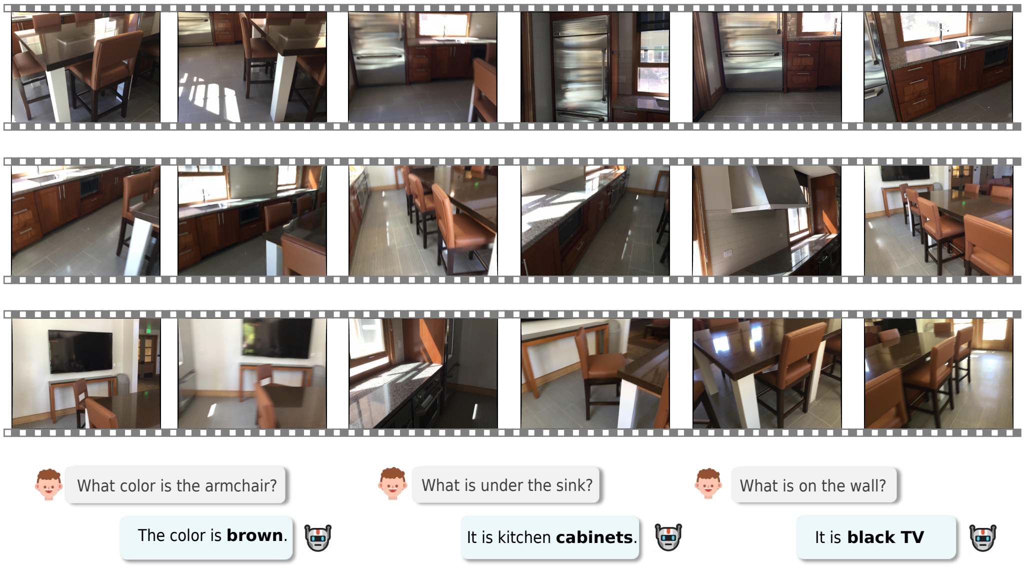

Figure 7: **Qualitive Results: Question Answering.** We provide videos without object annotations.

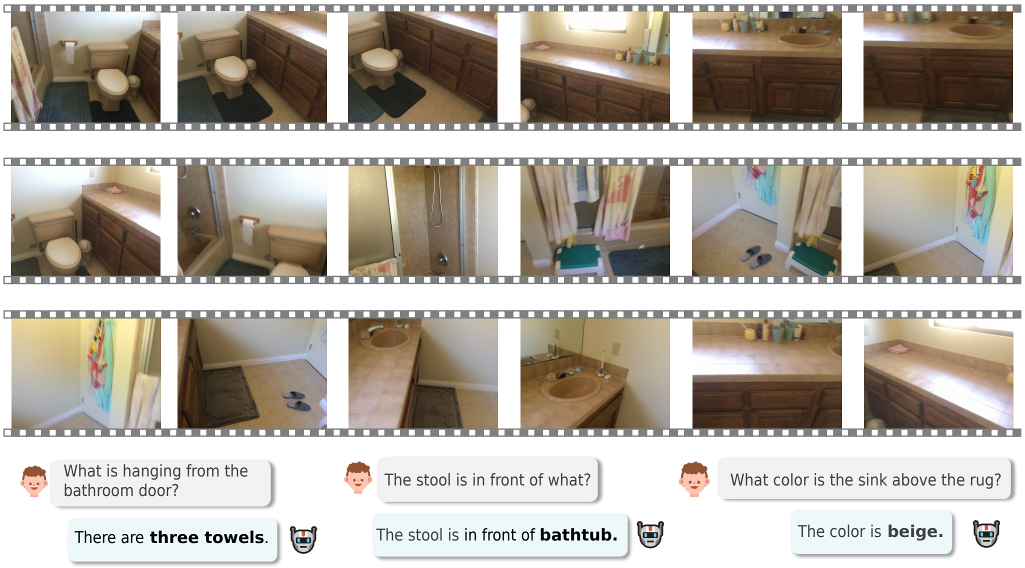
What is hanging from the bathroom door?
There are **three towels**.
The stool is in front of what?
The stool is in front of **bathtub.**
What color is the sink above the rug?
The color is **beige.**

Figure 8: **Qualitive Results: Question Answering.** We provide videos without object annotations.

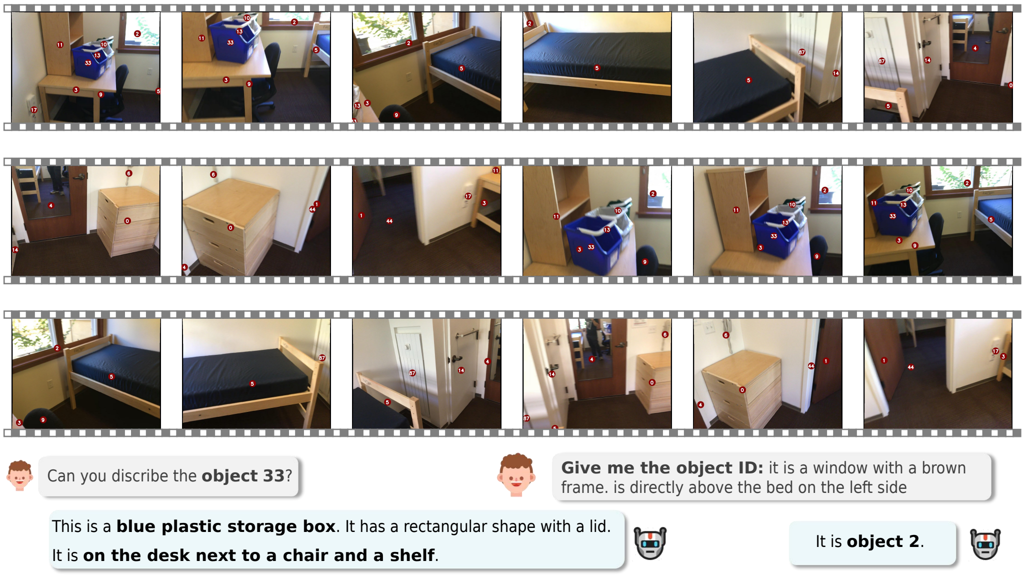

Can you discribe the **object 33**?

This is a **blue plastic storage box**. It has a rectangular shape with a lid. It is **on the desk next to a chair and a shelf**.

Give me the object ID: it is a window with a brown frame. is directly above the bed on the left side

It is **object 2**.

Figure 9: **Qualitive Results: 3D Dense Caption and Visual Grounding.** We provide videos with object annotations.

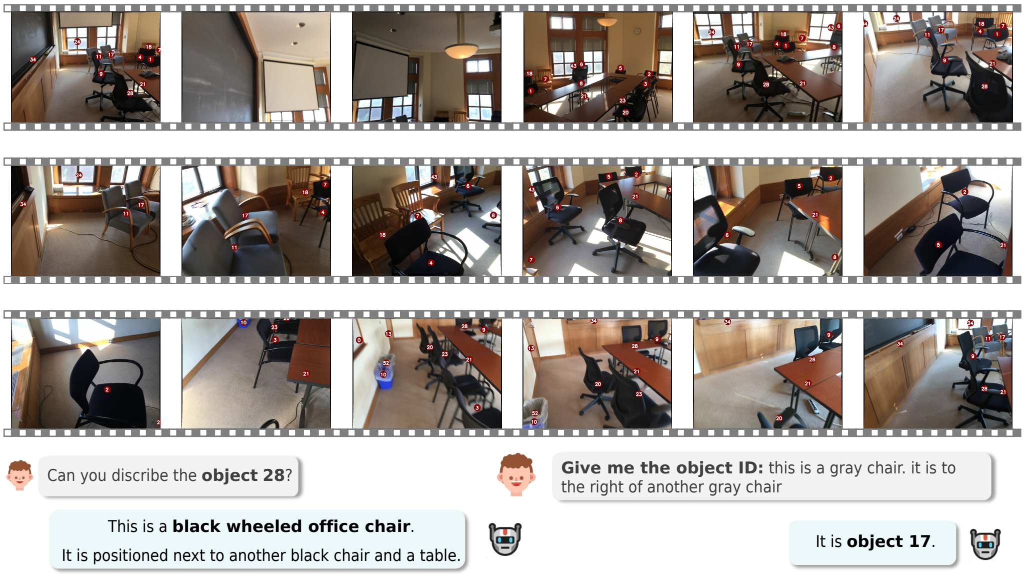

Can you discribe the **object 28**?

This is a **black wheeled office chair**. It is positioned next to another black chair and a table.

Give me the object ID: this is a gray chair. it is to the right of another gray chair

It is **object 17**.

Figure 10: **Qualitive Results: 3D Dense Caption and Visual Grounding.** We provide videos with object annotations.

F Original Related work

3D indoor scene understanding. 3D indoor scene understanding allows robots to identify object positions, structures, and relationships within indoor environments, enabling question-and-answer interactions about the scene's content. This process combines 3D perception with large language models (LLMs). 3D perception, as a foundational component, is typically trained on common indoor datasets Dai et al. (2017a); Baruch et al. (2021); Chang et al. (2017); Mao et al. (2022); Ramakrishnan et al. (2021); Wald et al. (2019); Straub et al. (2019); Deitke et al. (2022); Khanna et al. (2024); Zheng et al. (2020) using point clouds as input, supporting tasks like 3D object detection and instance segmentation Qi et al. (2019); Jiang et al. (2020); Misra et al. (2021); Schult et al. (2023); Vu et al. (2022); Wu et al. (2024b); Yunhan Yang (2023). Recent advancements in 3D Vision-Language Learning (3D-VL) combine 3D perception tasks with natural language, introducing diverse textual annotations on datasets like ScanNet to support tasks such as 3D Question Answering Azuma et al. (2022); Ma et al. (2023); Ye et al. (2022); Chen et al. (2022c), 3D Dense Captioning Chen et al. (2021), and 3D Visual Grounding Chen et al. (2020); Zhang et al. (2023c); Achlioptas et al. (2020); Abdelreheem et al. (2024); Kang et al. (2024b). Initial studies focus on single 3D-VL tasks Yuan et al. (2022); Chen et al. (2023b); Wu et al. (2023); Bakr et al. (2022); He et al. (2021); Huang et al. (2022b); Jain et al. (2022); Luo et al. (2022); Yang et al. (2021); Zhao et al. (2021); Guo et al. (2023b), while recent research introduces unified models for multiple tasks Cai et al. (2022); Chen et al. (2022a). 2D vision-language pretraining (2D-VLP) has driven progress in 3D visual-language learning (3D-VL) Ha & Song (2022); Hegde et al. (2023); Peng et al. (2023a); Takmaz et al. (2023); Xue et al. (2023); Zhang et al. (2022; 2023b); Xu et al. (2024a), with recent 3D-VLP Zhu et al. (2023b; 2024b); Jin et al. (2023); Ding et al. (2023); Yang et al. (2023); Jia et al. (2024); Wang et al. (2024b) methods demonstrating that combining 2D visual cues with 3D point clouds enables complementary cross-modal alignment. This multimodal approach helps overcome geometric complexity and sparse annotation challenges in pure point processing.

3D Point cloud LLMs. 3D vision-language tasks aim to integrate 3D scene understanding with natural language processing. However, we aspire to go further by incorporating 3D content into large language models (LLMs) to achieve more natural human-computer interaction. Initially, this began with 3D point cloud LLMs. 3D point cloud LLMs take point clouds as input, enabling natural language generation and interaction in 3D scenes. Early 3D LLMs focused on object-level geometry and appearance Guo et al. (2023a); Qi et al. (2024b); Xu et al. (2024b); Qi et al. (2024a). Later, they expanded to indoor scenes, emphasizing spatial relationships among objects and overall scene features, often utilizing scene point clouds augmented with auxiliary 2D multi-view images Hong et al. (2023); Chen et al. (2024b); Wang et al. (2023c); Fu et al. (2024b); Man et al. (2024). To better capture object relationships, recent 3D LLMs decouple scene objects before feeding them into LLMs Huang et al. (2023b; 2024a). Some approaches rely more heavily on visual inputs to determine scene context Chandrasegaran et al. (2024); Zhu et al. (2024a); Liu et al. (2024a). Here, we aim to explore whether pure visual inputs can better handle indoor scene understanding.

Vision Language Models (VLMs). Vision Language Models (VLMs) are multimodal models that integrate visual and language processing capabilities, enabling the understanding and generation of combined image-text information. The origin of VLMs can be traced back to CLIP's 2D image-text pair pretraining Radford et al. (2021); Changpinyo et al. (2021); Schuhmann et al. (2022), which laid the foundation for incorporating LLMs. Early VLMs used attention mechanisms or Q-Former to fuse image and text modalities before inputting them to LLMs Li et al. (2022; 2023a); Dai et al. (2023); Alayrac et al. (2022); Huang et al. (2024b). Later, an approach emerged that directly projects image features into the LLM using an MLP Liu et al. (2023; 2024b); Li et al. (2024); Zhu et al. (2023a); Wang et al. (2024a), achieving better performance. Building on this, VLMs expanded into visual grounding tasks Wang et al. (2023a); Peng et al. (2023b); Rasheed et al. (2023); Lai et al. (2024); Dong et al. (2024); Sun et al. (2023); Chen et al. (2023a) and further to video understanding by using spatiotemporal compression to process information from long image sequences Zhang et al. (2023a); Cheng et al. (2024); Maaz et al. (2023); Luo et al. (2023); Ataallah et al. (2024); Li et al. (2023c); Song et al. (2023); Ren et al. (2023); Liu et al. (2024c). Currently, while some studies employ VLMs for indoor scene understanding, most remain either benchmark-oriented Yang et al. (2025); Li et al. (2025) or still rely on 3D-based methods Zhang et al. (2024); Zheng et al. (2025). This fundamentally reveals that VLMs cannot directly comprehend 3D scenes, making our core mission to empower them with 3D world interpretation capabilities.

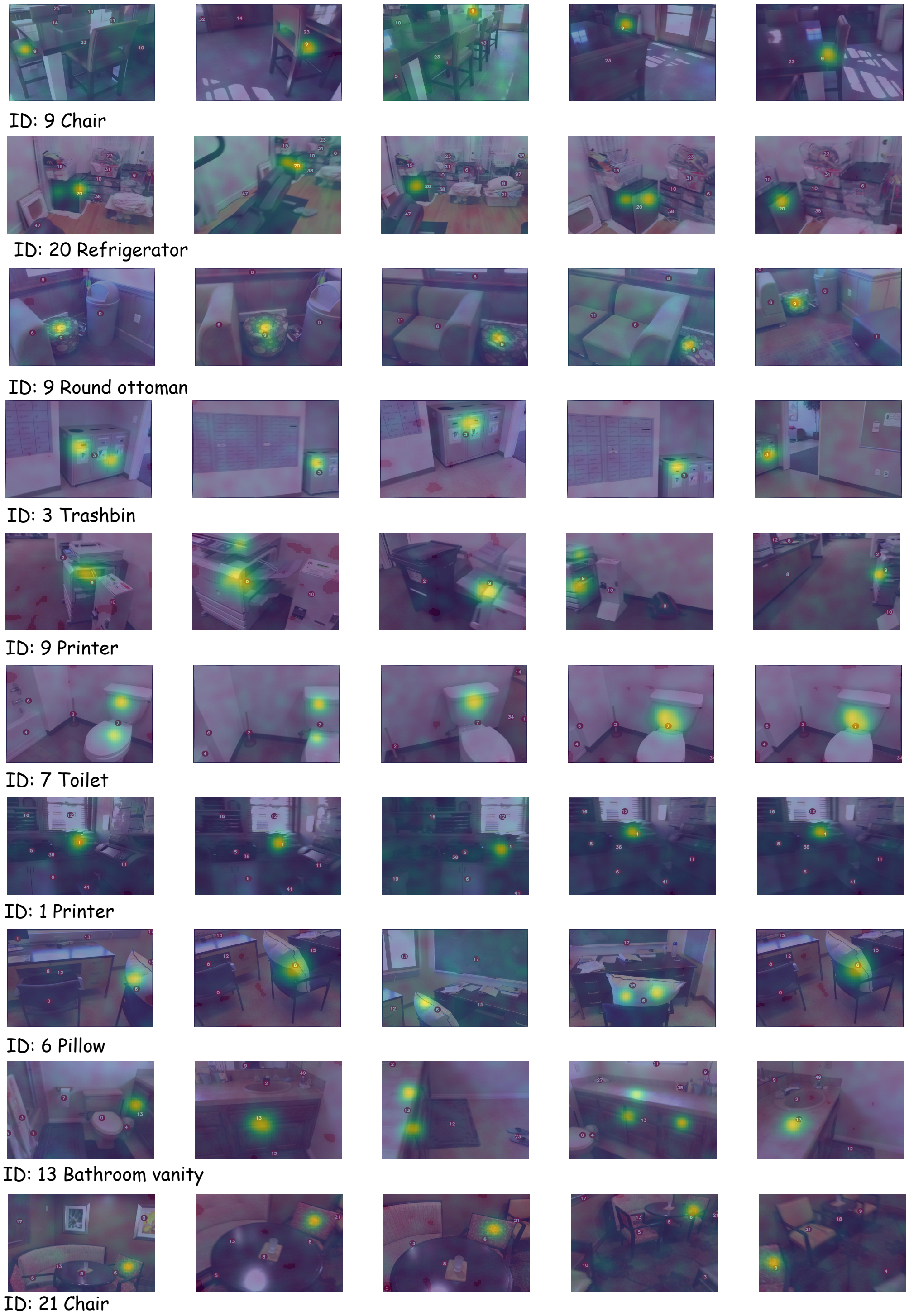

ID: 9 Chair

ID: 20 Refrigerator

ID: 9 Round ottoman

ID: 3 Trashbin

ID: 9 Printer

ID: 7 Toilet

ID: 1 Printer

ID: 6 Pillow

ID: 13 Bathroom vanity

ID: 21 Chair

Figure 11: **The heatmap after about the VLM feature.**

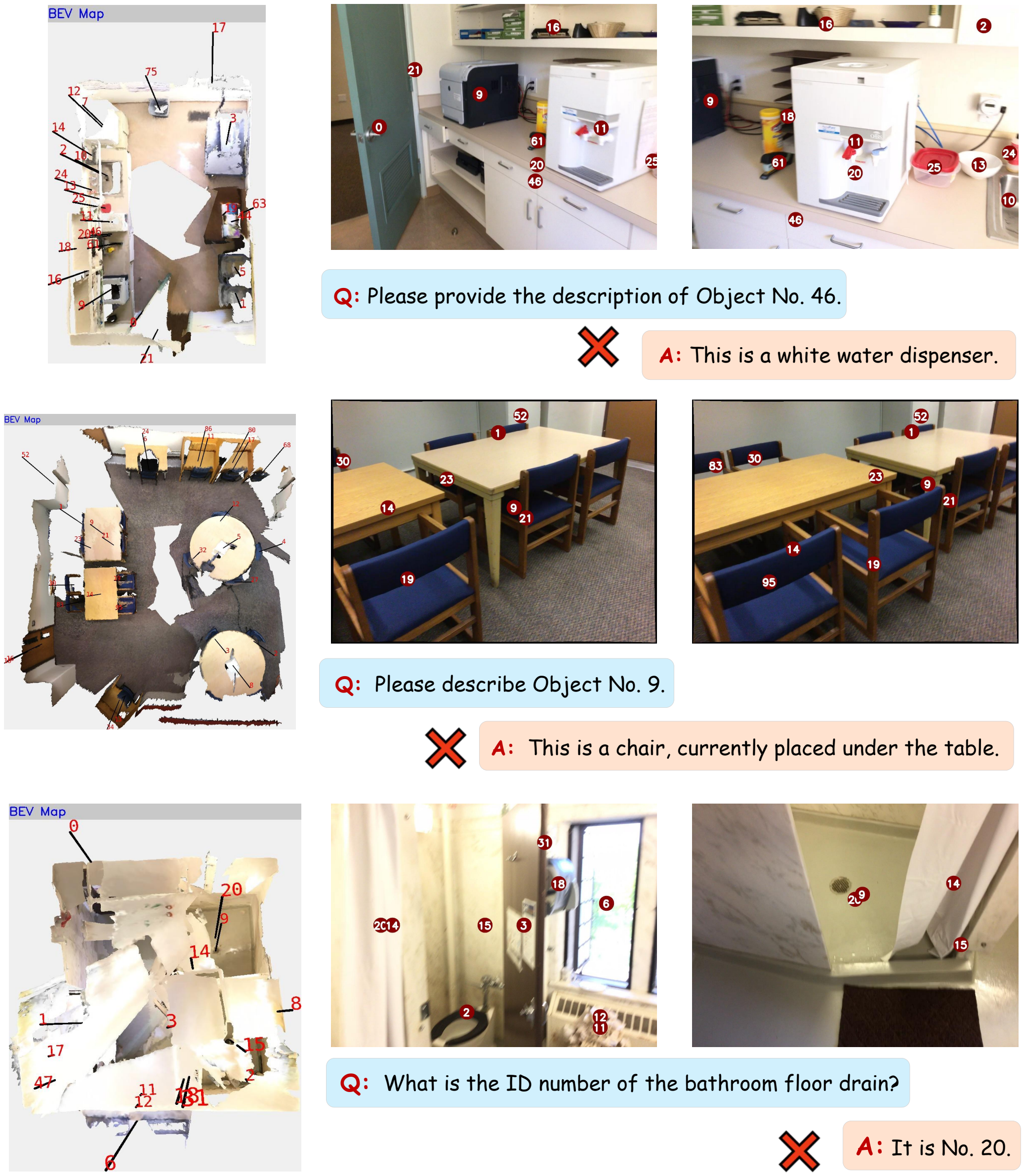

Q: Please provide the description of Object No. 46.

A: This is a white water dispenser.

Q: Please describe Object No. 9.

A: This is a chair, currently placed under the table.

Q: What is the ID number of the bathroom floor drain?

A: It is No. 20.

Figure 12: **Failure Cases of GPT4Scene.**